



Energy, Mines and
Resources Canada

Énergie, Mines et
Ressources Canada

Earth Physics Branch

Direction de la physique du globe

1 Observatory Crescent
Ottawa Canada
K1A 0Y3

1 Place de l'Observatoire
Ottawa Canada
K1A 0Y3

Geothermal Service of Canada

Service géothermique du Canada

TRANSIENT ELECTROMAGNETIC SURVEY TO MAP THE DISTRIBUTION
OF PERMAFROST AT DRAKE POINT, MELVILLE ISLAND, N.W.T.

GEO-PHYSI-CON Co. Ltd.
Calgary, Alberta

Earth Physics Branch Open File Number 83-16
Dossier public de la Direction de la Physique du Globe No. 83-16
Ottawa, Canada

NOT FOR REPRODUCTION

REPRODUCTION INTERDITE

Department of Energy, Mines &
Resources Canada
Earth Physics Branch
Division of Gravity, Geothermics
and Geodynamics

Ministère de l'Énergie, des
Mines et des Ressources du Canada
Direction de la Physique du Globe
Division de la gravité, géothermie
et géodynamique

62 Pages
Price: \$18.00

This document was produced
by scanning the original publication.

Ce document est le produit d'une
numérisation par balayage
de la publication originale.

ABSTRACT

A survey using transient electromagnetic sounding methods was carried out on the Sabine Peninsula, Melville Island, N.W.T. The purpose was to evaluate the technique for characterisation of permafrost conditions in the High Arctic, where in contrast with the Beaufort area the rocks are largely consolidated. In the Sabine area the high density of geothermal wells provided good control for the interpretation. The survey revealed a permafrost thickness ranging from 100m at the shoreline to 180m at a site 7 km inland. In comparison the depth of the 0°C isotherm ranges from 140 to 260m; the difference reflects the fine-grained nature of the sediments.

RESUME

Une méthode utilisant des sondages électromagnétiques transitoires a été réalisée sur la péninsule Sabine, île de Melville, T.N.O.. Son but était l'évaluation de la capacité de cette méthode géophysique d'établir le caractère du pergélisol dans le Grand Nord où, en opposition avec la région de mer Beaufort, les roches sont en général consolidées. Le grand nombre de sondages géothermiques dans la région de la péninsule permet une bonne commande de l'interprétation. Cette étude indique une épaisseur de pergélisol qui varie de 100m sur le littoral à 180m, 7 km à l'intérieur de la péninsule. En comparaison, la profondeur de l'isotherme 0°C varie de 140 à 260m; cette différence est attribuable au caractère fin des sédiments.

GEO-PHYSI-CON

TEM SURVEY TO MAP
THE DISTRIBUTION OF PERMAFROST
DRAKE POINT, MELVILLE ISLAND, N.W.T.

Prepared For

DEPT. OF ENERGY, MINES & RESOURCES
EARTH PHYSICS BRANCH
OTTAWA, ONTARIO

Prepared By

GEO-PHYSI-CON CO. LTD.
CALGARY, ALBERTA

June 1983
C83-16

GEO-PHYSI-CON

TABLE OF CONTENTS

	Page
1.0 INTRODUCTION	1
2.0 LOGISTICS	2
3.0 DATA ACQUISITION	2
4.0 INSTRUMENTATION AND THEORY	5
4.1 EM37 - Transient System	6
4.2 EM31 and EM34-3 - Fixed Frequency Systems	17
5.0 INTERPRETATION METHODS	20
5.1 General	20
5.2 Relative and Absolute Coordinates	21
5.3 The Description of Apparent Resistivity Curves	22
5.4 Distortions of the Apparent Resistivity Curves	23
5.5 Fixed Frequency EM Data	24
6.0 RESULTS	25
7.0 CONCLUSIONS AND RECOMMENDATIONS	27
REFERENCES	31
APPENDIX A - Manufacturer's Specifications for Geonics EM31, EM34-3 and EM37	

1.0 INTRODUCTION

During May, 1983 a geophysical test survey was carried out in the vicinity of Drake Point, Melville Island, N.W.T. The objective of the survey was to determine the ability of the transient electromagnetic sounding method (TEM) to measure the vertical and horizontal distribution of permafrost. In addition, fixed frequency electromagnetic (EM) measurements were taken to monitor lateral changes in the near surface sediments. Measurements were recorded along a 10 km line shown in Figure 1.

This report contains a detailed description of the logistics, data acquisition, results of the survey, and recommendations for future surveys.

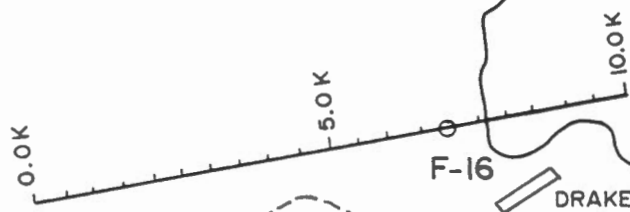
Authorization for the work was quoted by Dr. A. Judge (Earth Physics Branch) under contract number OSQ83-00022, dated May 12, 1983.

109° 76° 30' 108° 30' 76° 30'



BYAM MARTIN CHANNEL

DRAKE POINT



F-16

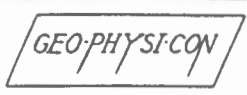
DRAKE AIRSTRIP

ROAD

o D-73

● PANARTIC MARRYATT CAMP K-71

LOCATION OF TEST SURVEY LINE



SCALE 1:125,000	DRAWN BY	DATE JUNE, 1983
NTS. 79 B	PROJECT NO. C 83-16	FIGURE 1

2.0 LOGISTICS

The test survey was performed by a three-man crew from May 20 to 23 and a four man crew from May 24 to 30, 1983. Mobilization and demobilization between Calgary and the Marryatt Camp took place on May 19 and 31, 1983.

The crew lodged at Panarctic Oils Ltd., Marryatt Camp, located approximately 15 km from the survey site. The crew travelled daily to and from the survey site by a 4-wheel vehicle. Once at the survey site the crew used 2 Alpine snowmobiles and a Bombardier Skidozer for ground transport and the moving of the TEM equipment from station to station. All vehicles were contracted to Geo-Physi-Con Co. Ltd. by Panarctic Oils Ltd.

3.0 DATA ACQUISITION

The TEM survey consisted of 21 sounding stations along a 10 km line at 500 metre intervals as shown in Figure 1. Of the 10 km surveyed approximately 7.6 km was on shore and 2.4 km off shore. For stations located off shore transmitter loop sizes of 500 by 500 metres and 100 by 100 metres were used. On shore

GEO-PHYSI-CON

the large loop size was changed to 400 by 400 metres. The large loop size was used to obtain data identifying the base of permafrost at each station. The small loop sizes were used to obtain data to better define shallow discontinuities which are less evident using the large loop.

A Geonics EM37 transient electromagnetic (TEM) system was used to carry out the survey. The manufacturer's specifications of the instrument are included in Appendix A. For stations on shore, measurements were taken using frequencies of 30 Hz and 3 Hz, while for stations off shore, measurements were taken using frequencies of 30 Hz, 3 Hz and 0.3 Hz.

Fixed frequency (EM) measurements were also taken along the survey line at 50m and 100m station intervals. The EM data were taken using the Geonics EM31 and EM34-3. The manufacturer's specifications of these instruments are also included in Appendix A.

Each of the instruments were used in 6 different measurement modes. Table 1 lists the exploration modes, station spacing and effective depths of exploration.

TABLE 1 - EM MEASUREMENT MODES RECORDED

MEASUREMENT MODE	STATION SPACING	EFFECTIVE EXPLORATION DEPTH
EM31VG - vertical coplanar loop mode at ground level	50 m	2.0
EM31HZ - horizontal coplanar loop mode at hip level	50 m	4.0
EM31HG - horizontal coplanar loop mode at ground level	50 m	5.0
EM34-20V - vertical coplanar loop mode, 20m loop separation	100 m	11.5
EM34-40V - vertical coplanar loop mode, 40m loop separation	100 m	23.0
EM34-40H - horizontal coplanar loop mode, 40m loop separation	100 m	50.0

4.0 INSTRUMENTATION AND THEORY

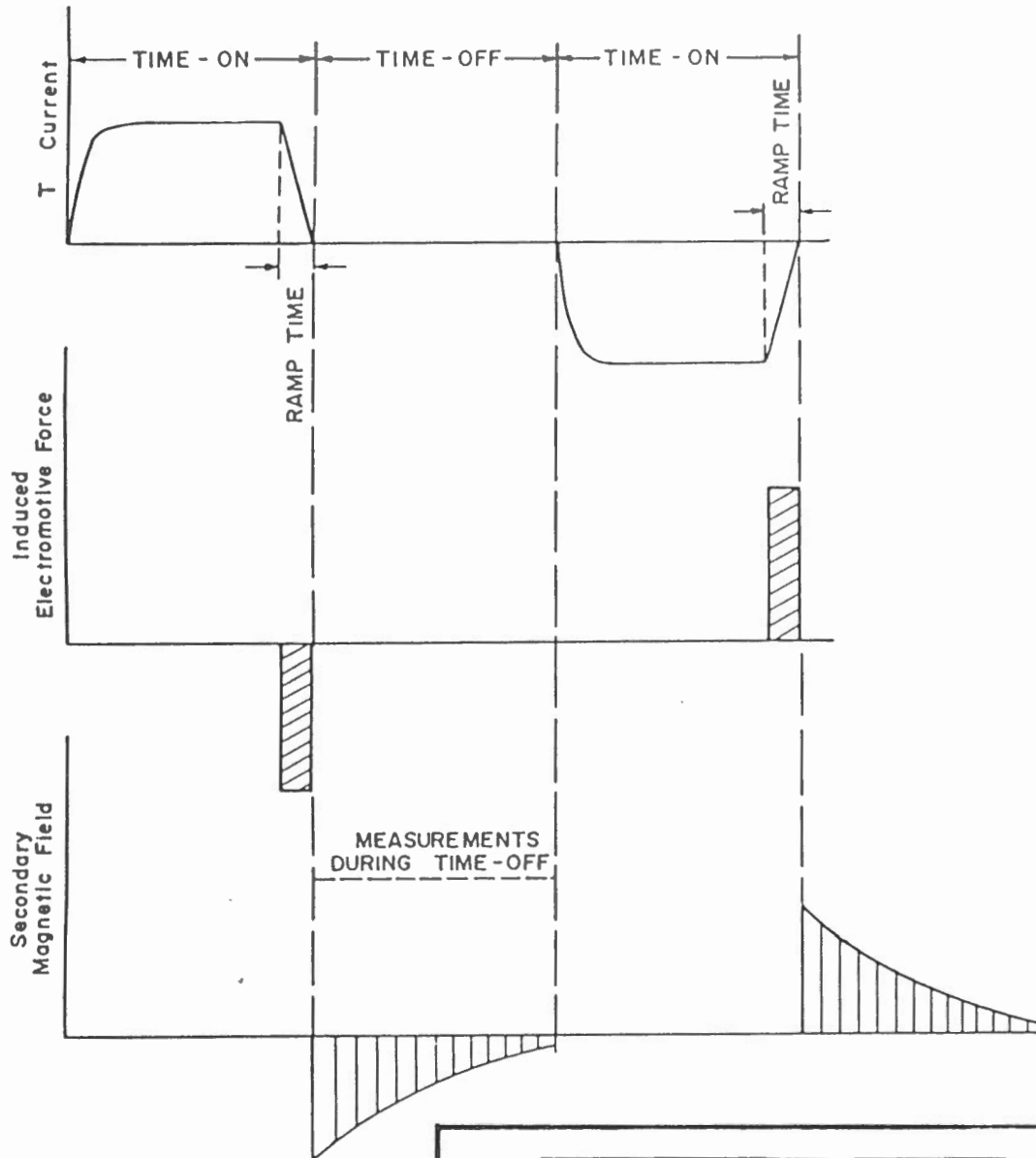
4.1 EM37 - Transient System

The transient system consists of a transmitter and receiver. The transmitter configuration used was a horizontal non-grounded loop. Figure 2 shows the behavior of the current wave form in the transmitter loop as a function of time. The system has equal periods of time-on and time-off. Three base frequencies for pulse repetition, 30 Hz (HF), 3 Hz (LF) and 0.3 Hz (VLF) can be employed. This gives time-on and time-off periods of 8.33 ms, 83.3 ms and 833 ms, respectively. The turn-on pulse is approximately of the form:

$$J(t) = J_0(1 - \exp(-t/\tau_0))$$

where $J(t)$ is the current at time t after turn-on,
 J_0 is the peak current, and
 τ_0 is an on-time constant.

The time constant τ_0 depends mainly on the size of the transmitter loop used and is approximately 0.5 millisecond for a 400 m by 400 m loop.



a) CURRENT IN TRANSMITTER LOOP

b) INDUCED ELECTROMOTIVE FORCE CAUSED BY T CURRENT

c) SECONDARY MAGNETIC FIELD CAUSED BY EDDY CURRENTS

GEO-PHYSI-CON

SYSTEM WAVEFORMS

GEO-PHYSI-CON

The turn-off ramp is linear. The ramp time is experimentally measured on the instrument. The ramp time is a function of transmitter loop size and peak current. It varies from approximately 150 microseconds for a 100 m by 100 m loops to 500 microseconds for the larger loops.

The receiving element is a multi-turn coil that measures the electromotive force caused by the time derivative of the secondary magnetic field. The receiver can occupy stations inside as well as outside the loop. For the present survey, measurements were made only with the receiver in the centre of the transmitter loop and at base frequencies of 30 Hz and 3 Hz.

Table 2 lists the positions and widths of the time gates of the receiver at high, low and very low frequency. The time is in reference to the bottom of the turn-off ramp (see illustration Table 2). To precisely reference the gate locations to the end of the ramp, the ramp time measured on the transmitter is set on the receiver.

Synchronization of the transmitter and receiver is achieved using high stability (oven controlled) quartz crystals. This method of synchronization requires phasing of the crystals

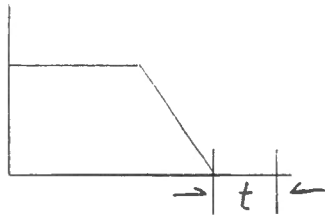


TABLE 2

List of Time of Gate Centres and Gate Widths

CHANNEL NO.	GATE CENTRE			GATE WIDTH		
	HF	LF	VLF	HF	LF	VLF
1	0.089 ms	0.89 ms	8.9 ms	0.018 ms	0.18 ms	1.8 ms
2	0.100	1.00	10.0	0.024	0.24	2.4
3	0.140	1.40	14.0	0.037	0.37	3.7
4	0.177	1.77	17.7	0.036	0.36	3.6
5	0.220	2.20	22.0	0.050	0.50	5.0
6	0.280	2.80	28.0	0.072	0.72	7.2
7	0.355	3.55	35.5	0.076	0.76	7.6
8	0.443	4.43	44.3	0.100	1.00	10.0
9	0.564	5.64	56.4	0.142	1.42	14.2
10	0.713	7.13	71.3	0.156	1.56	15.6
11	0.881	8.81	88.1	0.180	1.80	18.0
12	1.096	10.96	109.6	0.250	2.50	25.0
13	1.411	14.11	141.1	0.380	3.80	38.0
14	1.795	17.95	179.5	0.390	3.90	39.0
15	2.224	22.24	222.4	0.500	5.00	50.0
16	2.850	28.50	285.0	0.720	7.20	72.0
17	3.600	36.00	360.0	0.780	7.80	78.0
18	4.490	44.90	449.0	1.080	10.80	108.0
19	5.700	57.00	570.0	1.420	14.20	142.0
20	7.190	71.90	719.0	1.560	15.60	156.0

each time the transmitter frequency is changed or the transmitter is shut down. During transmitter shut down the oven temperatures are maintained for both the transmitter and receiver using the receiver battery pack.

Detailed manufacturer's specifications on the instrument are given in Appendix A.

4.1.1 Definition of Apparent Resistivity

It is common in electrical and electromagnetic prospecting (especially in soundings) not to work with the behavior of fields, but to convert the measured field components into apparent resistivities. This approach has also been used for many years in transient electromagnetic soundings.

It has been shown that the system, consisting of a square transmitter loop with the receiver at its centre, is completely equivalent in the time range employed to a system consisting of a magnetic dipole transmitter and electric dipole receiver. As a result, the theory developed for the latter case above is valid for the system used, provided that the distance between the dipoles is equal to $1/\sqrt{\pi}$ L, where L is the length of a side of the transmitter loop.

GEO-PHYSI-CON

To understand the definitions of apparent resistivity used in this report, consider the behavior of the field induced in a homogeneous half-space. In Figure 3 the tangential electrical field component is plotted versus the parameter, \mathcal{T}/r ,

where
$$\mathcal{T} = \sqrt{2\pi\rho t 10^7} \quad [1]$$

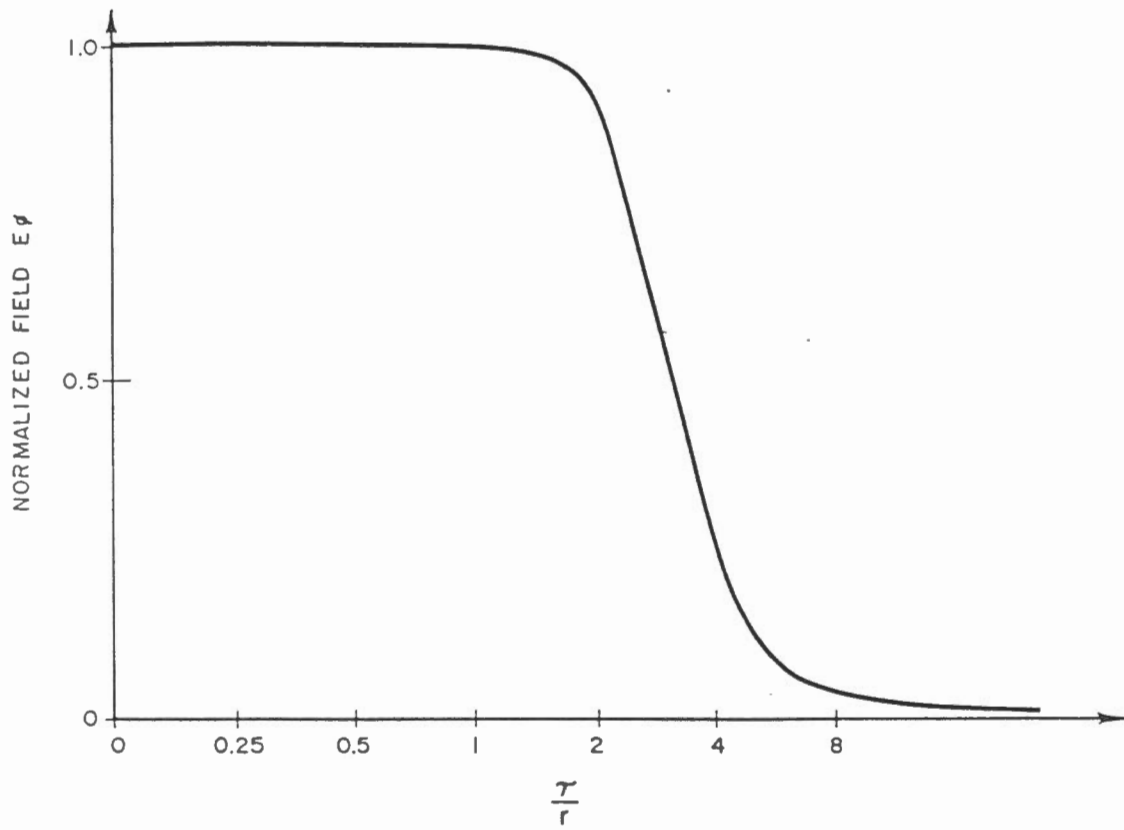
r = distance between transmitting dipole and point of measurement in metres,

ρ is the resistivity of half-space in ohm-m, and

t is time after turn-off in seconds

The general behavior of the field is a complex function, but it has been shown that at values of $\mathcal{T}/r < 2$, and at $\mathcal{T}/r > 10$, simple asymptotic expressions describe the field to good accuracy (5%). At early stage ($\mathcal{T}/r < 2$) the field is independent of time and the asymptotic expression is given by:

$$E_{\theta} = \frac{3m\rho}{2\pi r^4} \quad [2]$$



GEO-PHYSI-CON

ENGINEERING GEOPHYSICAL CONSULTANTS

BEHAVIOR OF E_ϕ

C83-16

Figure 3

where m is the moment of the transmitting dipole in amperes- m^2 .

At late stage ($\tau/r > 10$) the field is given by the expression:

$$E_{\phi} = \frac{m r \mu^{5/2}}{40\pi^{3/2} \rho^{3/2} t^{5/2}} \quad [3]$$

where μ is magnetic susceptibility of free space in henry/m.

Clearly, two different definitions of apparent resistivity can be introduced from equations 2 and 3, i.e.

early stage definition $\rho = \frac{2\pi r^4}{3m} E_{\phi} \quad [4]$

late stage definition $\rho = \frac{\mu}{4\pi t} \left(\frac{r \mu m}{5t E_{\phi}} \right)^{2/3} \quad [5]$

For the present work both the early and the late stage expressions for defining apparent resistivity were used. Late

GEO-PHYSI-CON

stage behavior appears relatively quickly in the resistive on shore environments surveyed. Early stage behavior was observed where near surface sediments are extremely conductive (offshore environments). Thus, for the off shore stations early stage curves showed the variations in resistivity in the shallow subsurface and late stage curves were used to obtain information on deeper structures.

The interpretation of transient data mainly consists of comparing the measured apparent resistivity curves to curves computed for certain models of horizontally layered geoelectric sections. For this work, many theoretical apparent resistivity curves were calculated using specially developed computer programs. The algorithms of the computer programs are subject to the following assumptions:

- a) the half-space is horizontally layered
- b) the current in the transmitting dipole is a perfect step function

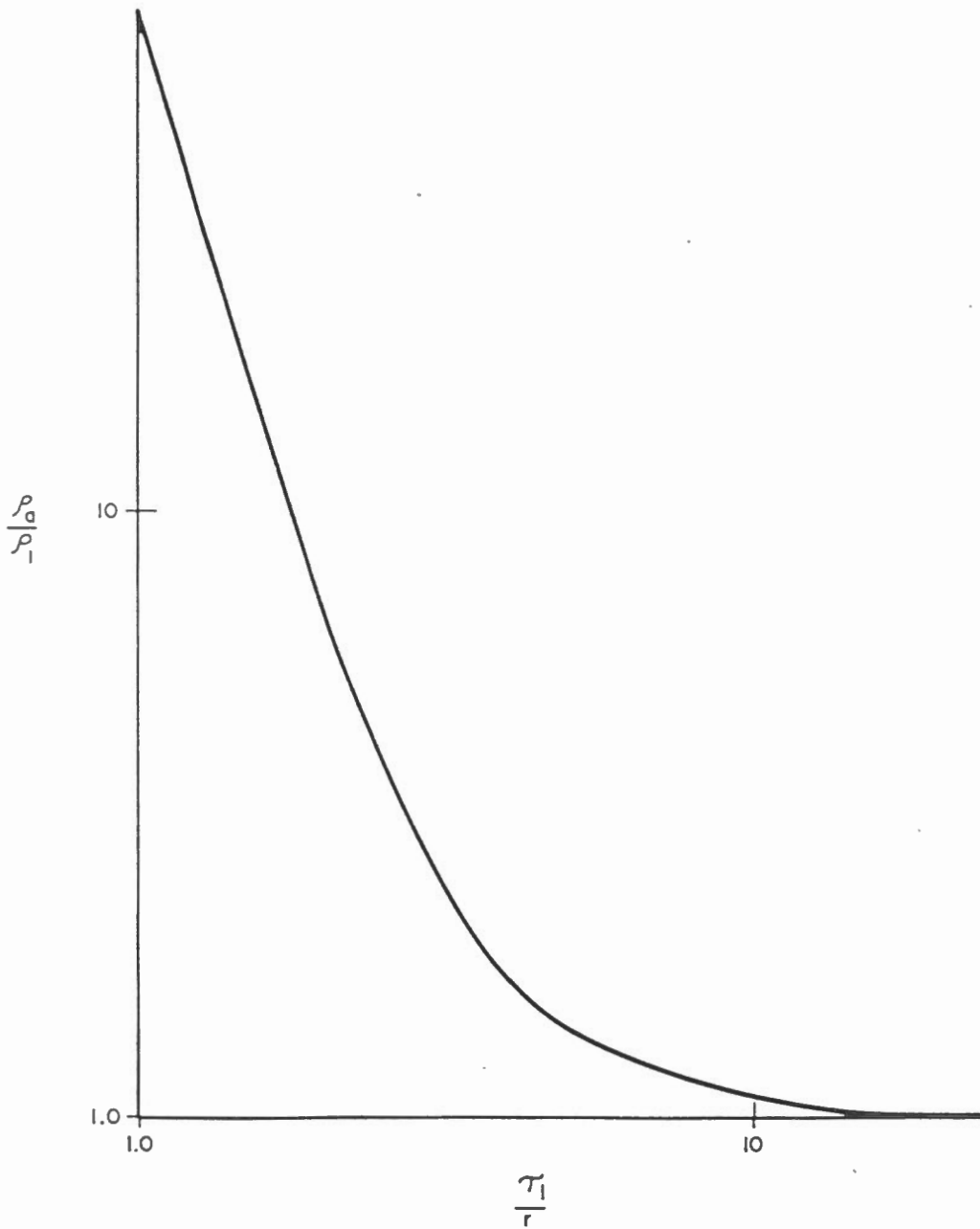
GEO-PHYSI-CON

To understand the behavior of the apparent resistivity curves generated by using the definition of equation 5, consider the two examples given in Figures 4 and 5. Figure 4 is for homogeneous half-space of resistivity ρ_1 ; on the vertical axis is plotted the ratio of ρ_a/ρ_1 and on the horizontal axis the parameter τ_1/r . It can be seen that when $\tau_1/r > 10$, ρ_a/ρ_1 approaches 1, i.e. the apparent resistivity measured approaches the true resistivity of the half-space. In practice measurements are made at constant r . The true resistivity is measured when

$$t > \frac{r^2}{2 \pi \rho 10^5}$$

At values of $\tau/r < 10$, the values of ρ_a/ρ_1 can be seen to rapidly increase with decreasing τ/r . This is caused by the fact that the field, E_0 , at early time can no longer be described by the late stage asymptotic expression of equation 3. However, it can be expressed using the early stage asymptotic expression of equation 2.

Figure 5 shows late stage apparent resistivity curves for two layer sections when $\rho_2/\rho_1 < 1$. The resistivity stratification for the curves in Figure 5 could, for example, represent frozen ground underlain by unfrozen ground. On the horizontal



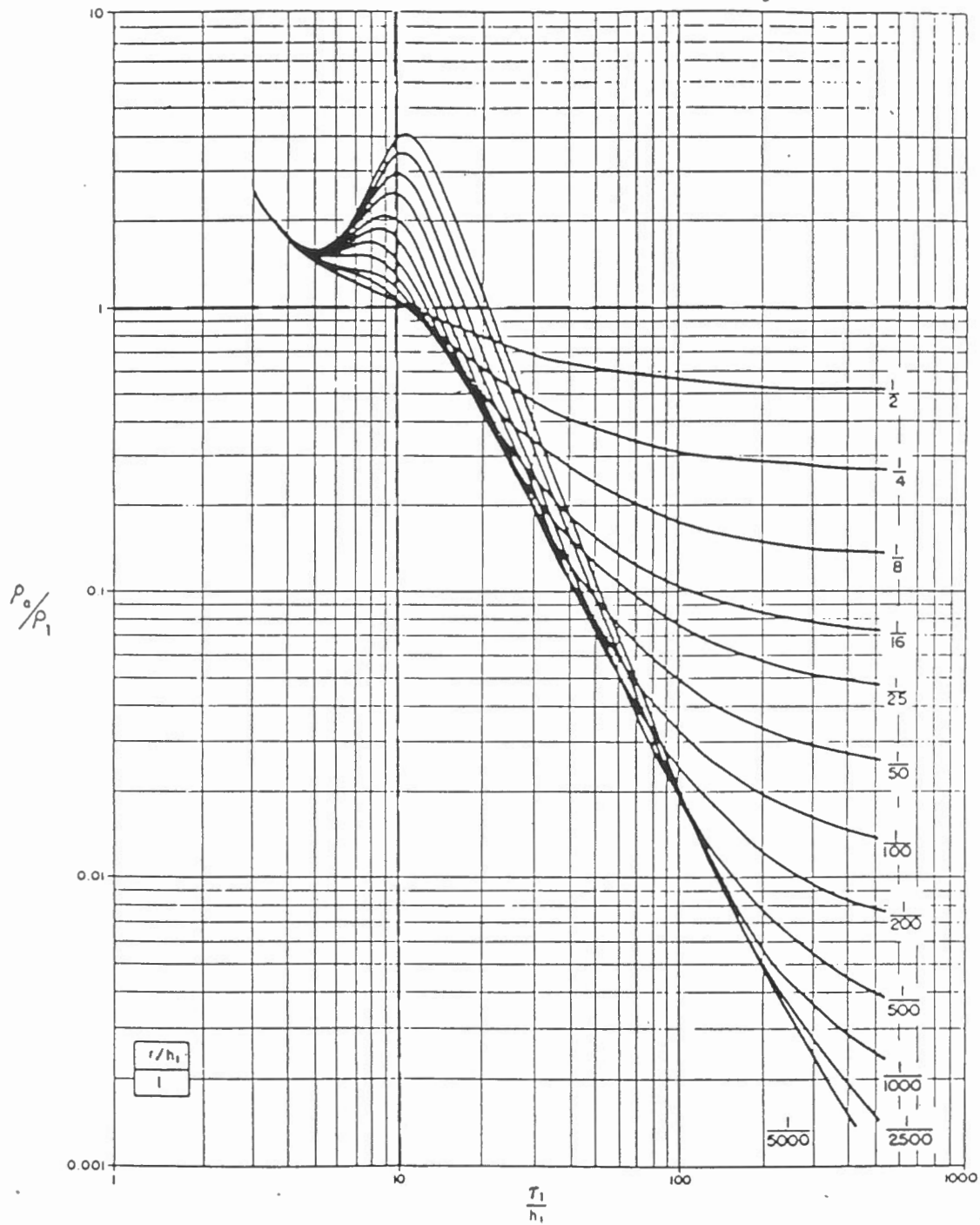
GEO-PHYSI-CON

ENGINEERING GEOPHYSICAL CONSULTANTS

MASTER CURVE
HOMOGENEOUS HALF-SPACE

C83-16

Figure 4



GEO-PHYSI-CON

ENGINEERING GEOPHYSICAL CONSULTANTS

MASTER CURVE
TWO-LAYER MEDIUM

C83-16

Figure 5

axis, the parameter τ_1/h_1 is plotted, where h_1 is the thickness of the first layer (frozen ground). The main features of the apparent resistivity curves are:

- a) At small values of the abscissa all curves merge into one corresponding to the behavior of uniform half-space of resistivity, ρ_1 .
- b) At values of $8 < \tau_1/h_1 < 10$, the apparent resistivity curves for sections with $\rho_2/\rho_1 < 1/16$ and $r/h_1 \leq 1$ have a maximum.
- c) At values of $\tau_1/h_1 > 10$, there are descending branches. For values of $\rho_2/\rho_1 < 1/16$ the descending branches have parallel segments.
- d) At large values of τ_1/h_1 , the apparent resistivity curves approach ρ_2 .

4.1.2 Correction Factors for Ramp Time

It was stated in Section 4.1.1 that the master curves are computed for a perfect step function. The transmitter current

GEO-PHYSI-CON

when turned off has a finite ramp time (Section 4.1). To make the measured apparent resistivity curve correspond to the master curves a correction must be made for the ramp turn off. The correction factors that are often used are based on either the late stage behaviour of the field or the full expression of the field for a homogenous half-space. In resistive environments (on shore) the late stage expression for the correction is used, as it is valid over the most of the time range employed. In conductive environments (off shore) the correction based on the full field expression is used, as late stage appears more slowly.

The late stage correction factors are based on the fact that, at late time, the field is proportional to $t^{-5/2}$, so that

$$\frac{Q(t)}{R(t)} = \frac{1}{\Delta T} \int_t^{t+\Delta T} t^{-5/2} dt \quad [6]$$

where $Q(t)$ is the field due to the linear ramp at a time, t ,
 ΔT is the ramp time, and
 $R(t)$ is the field measured due to a perfect step function at time, t .

The full expression correction factor is based on the relation:

$$E_{\phi} = \frac{3m\rho}{2\pi r^4} \left[\phi(u) - \sqrt{\frac{2}{\pi}} u \left(1 + \frac{u^2}{3}\right) e^{-\frac{u^2}{2}} \right] \quad [7]$$

where the parameter $u = \frac{2\pi\rho}{\tau}$,

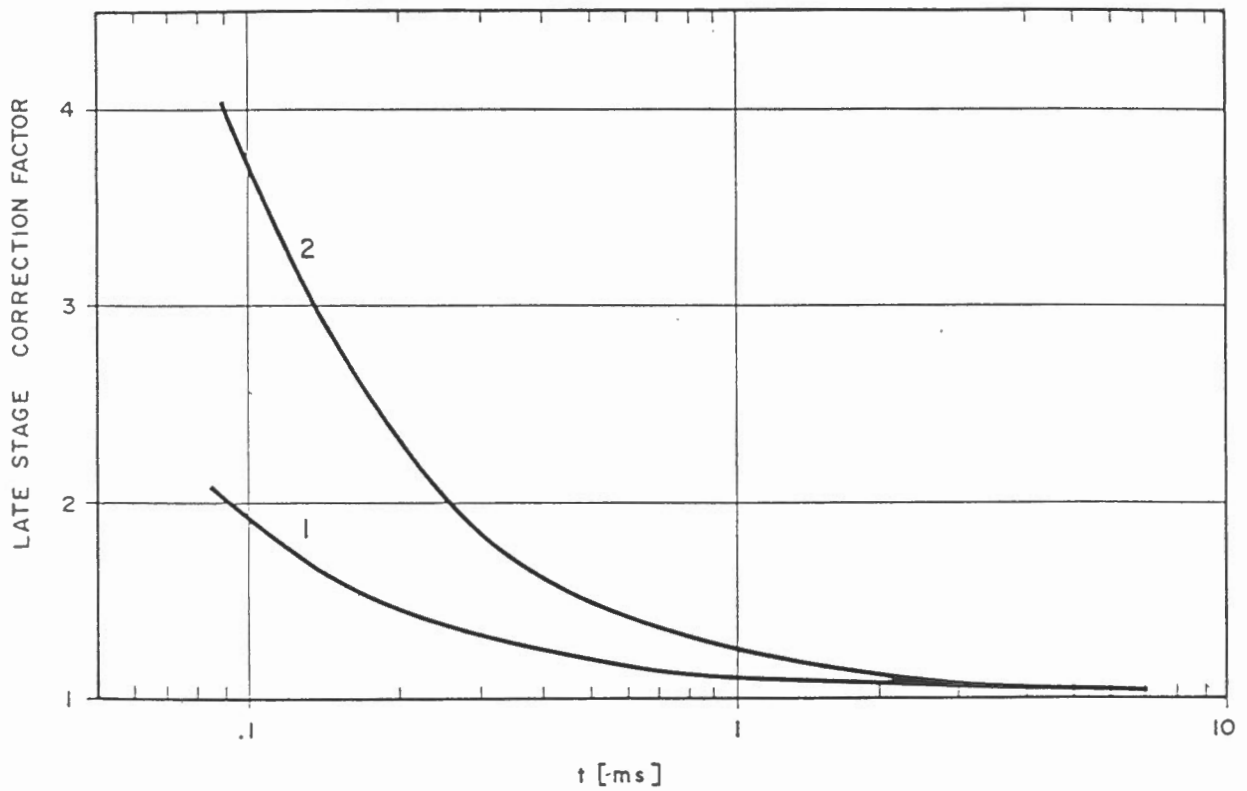
$\phi(u)$ is the error function,

$$\tau = \sqrt{2\pi\rho t 10^7} \quad ,$$

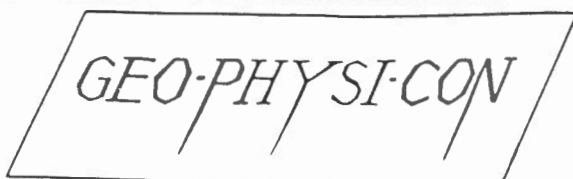
m is the transmitter dipole moment, and

ρ is the half-space resistivity.

In Figure 6 the late stage correction factor is plotted as a function of t for two values of ΔT . In Figure 7 the correction factor based on late stage and on the full expression for the field for a homogeneous half-space having a resistivity of 2 ohm-m are compared. In Figure 8, the difference in apparent resistivities, using the two different correction factors, is shown. The curves merge at the onset of late stage behavior.



- 1 Ramp time 70 microsec
- 2 Ramp time 200 microsec

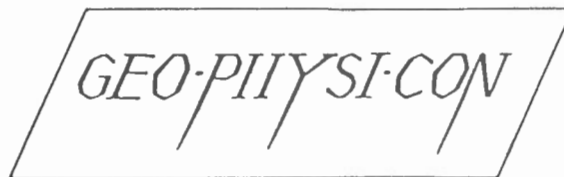
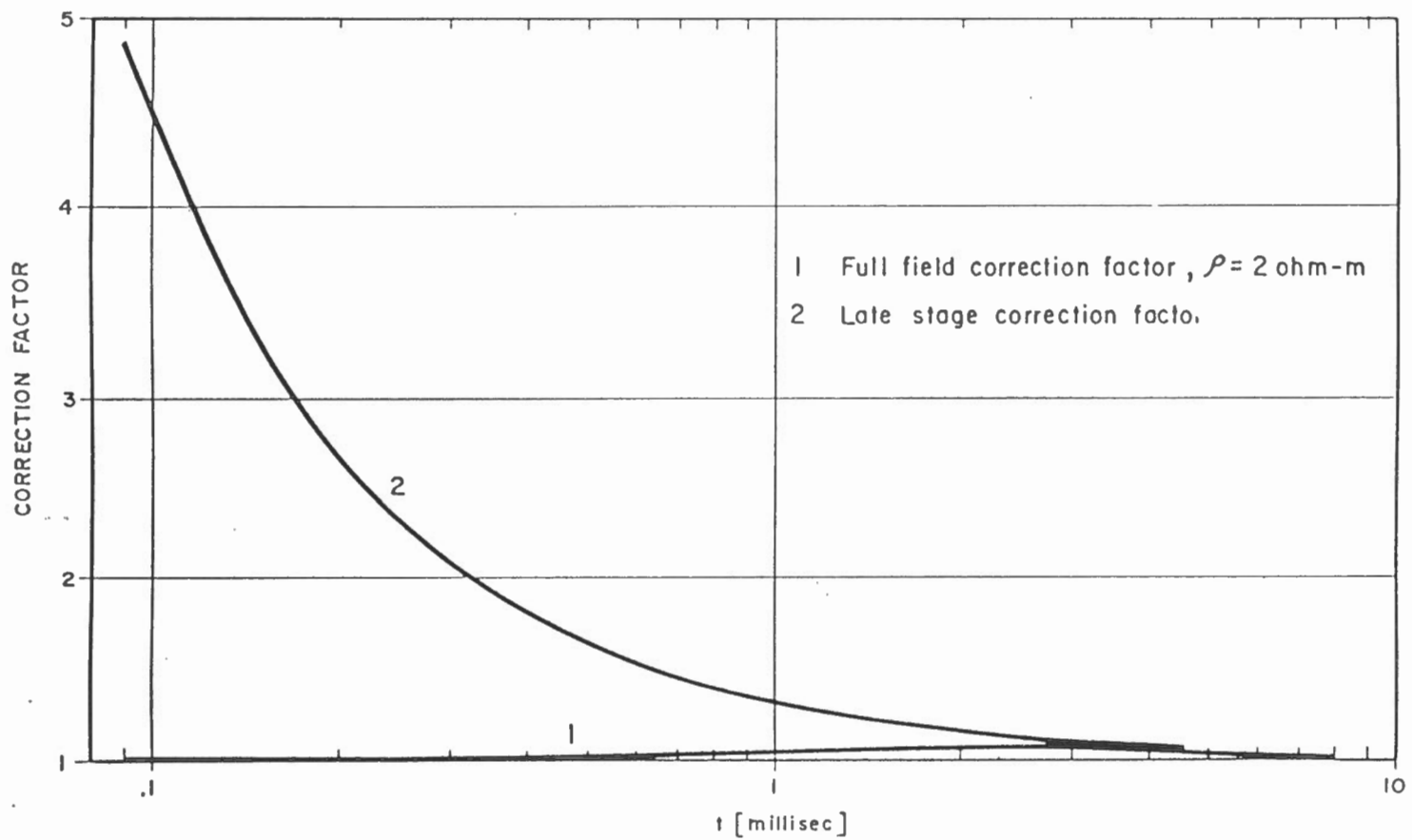


ENGINEERING GEOPHYSICAL CONSULTANTS

CORRECTION FOR RAMP TIME

C83-16

Figure 6

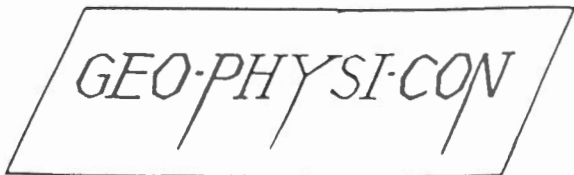
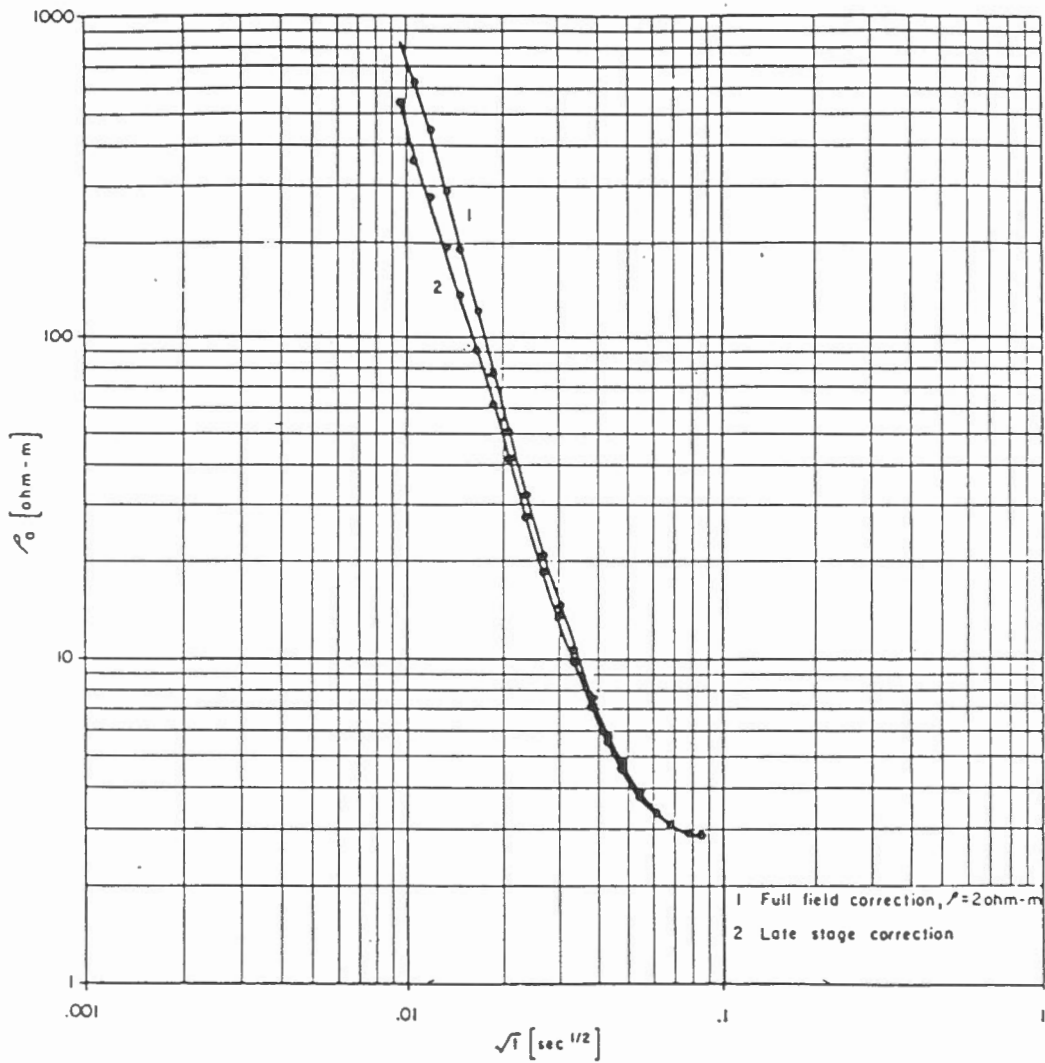


ENGINEERING GEOPHYSICAL CONSULTANTS

CORRECTION FACTORS
 FOR RAMP TIME (250 microsec)

C 83-16

Figure 7



ENGINEERING GEOPHYSICAL CONSULTANTS

APPARENT RESISTIVITY CURVES
 WITH DIFFERENT CORRECTION

C83-16

Figure 8

4.1.3 Influence of Turn-on Time and Ramp Time of Previous Pulse

The current waveform in the transmitter loop, as discussed in Section 4.1, consists of periods of time-on and time-off. The electromotive force in the receiver is measured only during time-off. The master curves are computed on the assumption that the secondary field is induced by the last ramp turn-off only. It is assumed that the secondary field, due to previous changes in current, has decayed to a negligible level.

It had been previously found that under certain conditions the turn-on time and ramp turn-off of a previous pulse can influence the measured secondary field. To investigate the influence of previous pulses the following were considered:

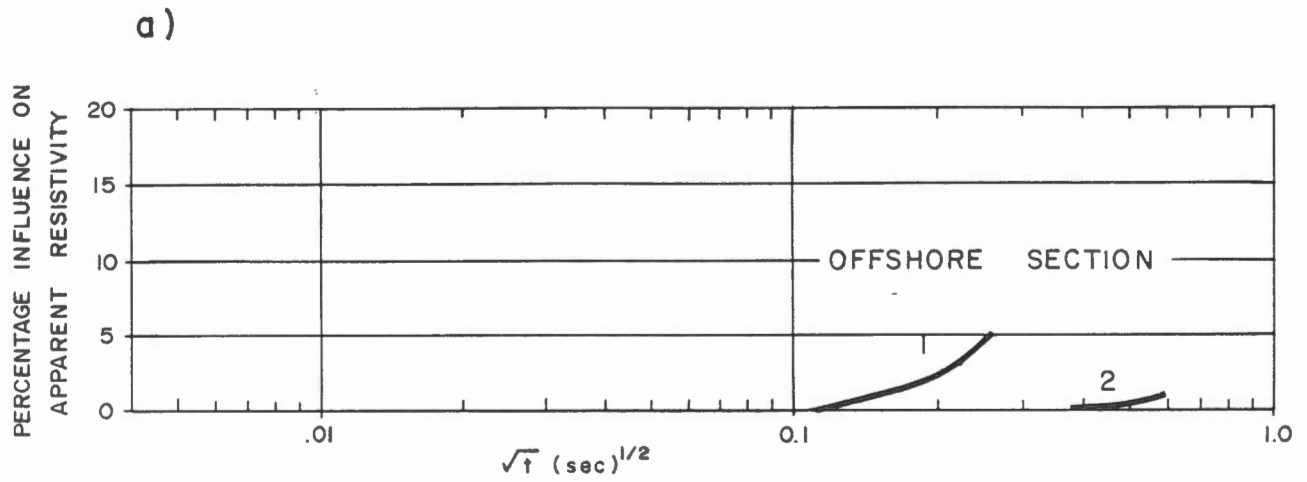
- i) for the field measured at time t the influence of turn-on occurs at $(t+8.3)$ ms for high frequency (HF, 30 Hz), and at $(t+83)$ ms at low frequency (LF, 3 Hz). The polarity of turn-on pulse is opposite in respect to turn-off ramp time.
- ii) the influence of the previous ramp turn-off occurs at $(t+2 \times 8.3)$ ms for high frequency, and at $(t+2 \times 83)$ ms at low frequency. The polarity of this pulse is also opposite to the main turn-off pulse.

iii) it is assumed that the amplitude of the induced electromotive force is the same for both turn-on and turn-off pulses.

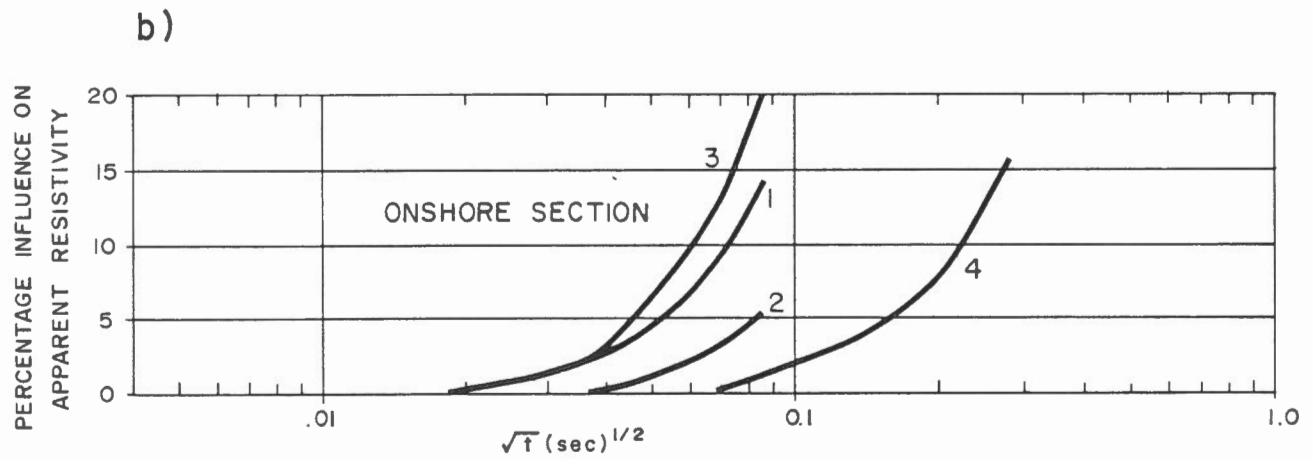
In Figure 9 the influence of the turn-on pulse on the apparent resistivity is computed from master curves for the geoelectric sections typical for both on shore and off shore environments. The computations are made for high, low and very low frequencies. The effect of pulse turn-on can be reduced by measurements at a lower frequency in the same time range, since the last ten time channels at a higher frequency are equivalent to the first 10 time channels at the lower frequency.

4.2 EM31 and EM34-3 - Fixed Frequency Systems

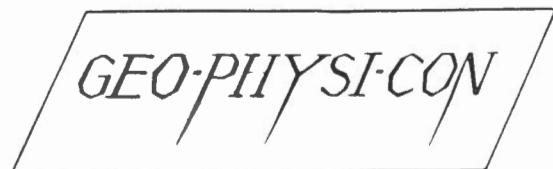
In the EM method eddy current flow is induced in the ground by the time varying magnetic field of a vertical or horizontal magnetic dipole transmitter operating at a fixed frequency. The eddy current flow induces a secondary magnetic field which, together with the primary field, is sensed by a similar receiver dipole. The ratio of the primary and secondary fields is related to the conductivity of the subsurface.



- 1 Turn-on Time for 3 Hz
- 2 Turn-on Time for .3 Hz



- 1 Turn-on Time for 30 Hz
- 2 Previous Turn-off Time for 30 Hz
- 3 Sum of 1 and 2
- 4 Turn-on Time for 3 Hz



INFLUENCE OF SUPERPOSITION OF PULSES

GEO-PHYSI-CON

The instrument parameters, frequency and coil separation, are selected so that operation can be described by the low induction number approximation. In this sense each induced eddy current loop is independent of the others and the measured (apparent) conductivity can be thought of as a linear superposition of the responses of strata within the exploration range of the array used.

Under certain restrictions concerning the maximum value of terrain conductivity the measured and strata conductivities are related by the following expression:

$$\sigma_a = \sum_{i=1}^n \sigma_i (R_i - R_{i-1}) \quad (8)$$

where σ_a is the apparent conductivity
 σ_i is the conductivity of the i th layer, and
 R_i, R_{i-1} are geometric (weighting) factors characteristic of the top and bottom of the i th layer.

The effective exploration depth of the EM equipment can be varied by changing one or more of loop spacing (s), loop orientation (vertical or horizontal), or height above terrain (h_0). All these parameters affect the distribution of the geometric factors. For horizontal coplanar loops geometric factors are described by

$$R(D) = (D^2 + 1)^{-1/2} \quad (9)$$

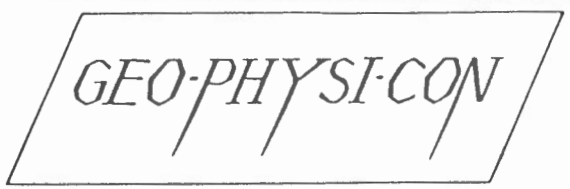
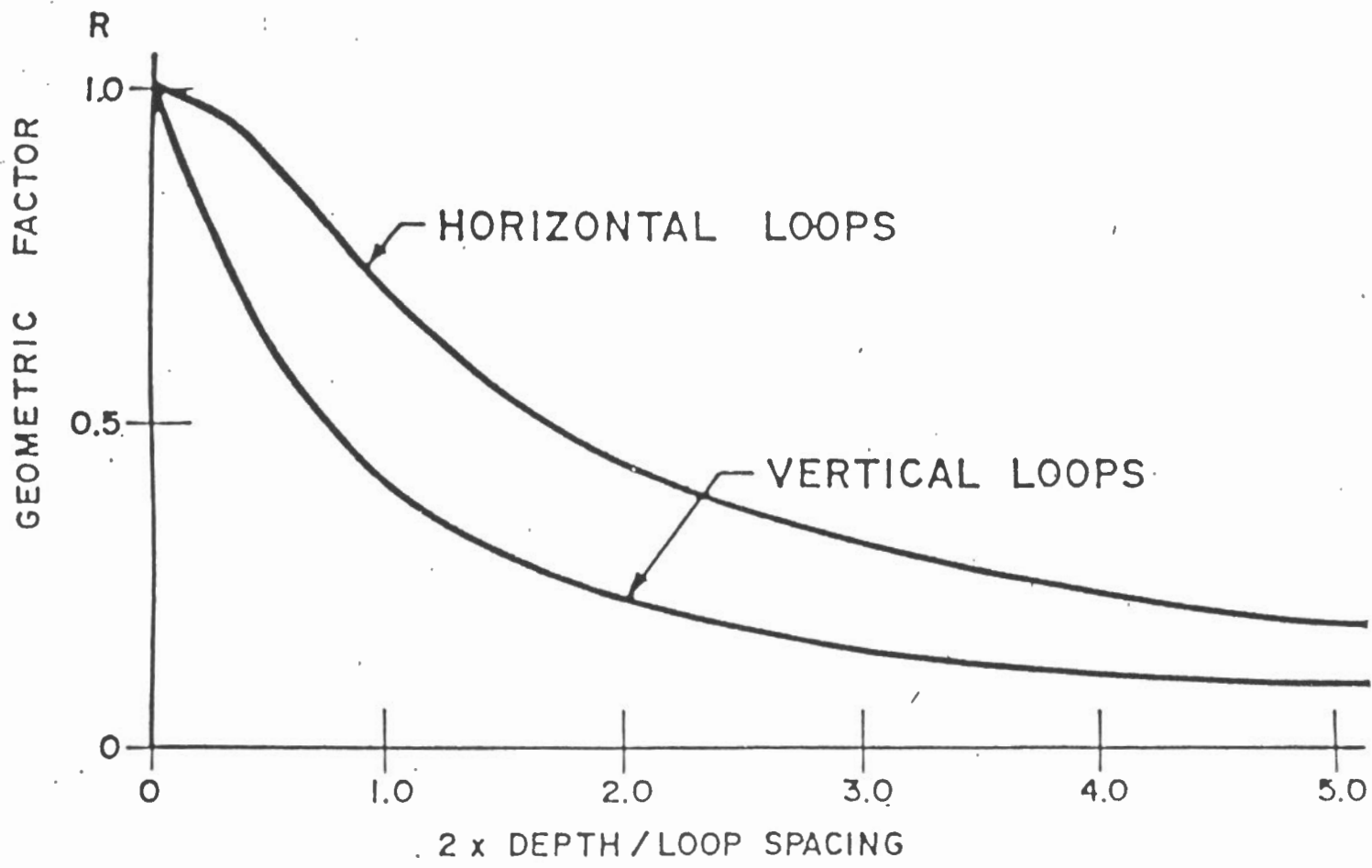
and for vertical coplanar loops

$$R(D) = [(D^2 + 1)^{1/2} - D] \quad (10)$$

where the parameter $D = 2(h_0 + d)/s$ (11)

and d is the depth below ground surface

A graph of the functions (9) and (10), above, is shown in Figure 10. From this figure it is evident that, for a common loop spacing, the horizontal loop mode senses effectively twice as deep as the vertical loop mode. The units of apparent conduc-



ENGINEERING GEOPHYSICAL CONSULTANTS

GEOMETRIC FACTORS FOR HORIZONTAL AND VERTICAL LOOPS

C 83-16

Figure 10

tivity used in this work are millimhos/metre. For the TEM method the units for apparent resistivity are ohm-metres. These are related by

$$(\text{mmho/m}) = (\text{ohm-m})^{-1} \times 10^3$$

Detailed manufacturer's specifications for the instruments used are given in Appendix A.

5.0 INTERPRETATION METHODS

5.1 General

Apparent resistivity curves have been prepared for data gathered using transmitter loop sizes of 100m by 100m and 400m by 400m or 500m by 500m for the late stage definition of apparent resistivity. Early stage apparent resistivity curves were also calculated for the 500m by 500m loops. The apparent resistivity curves obtained show two basic geoelectric sections corresponding to the on shore and off shore environments.

The fact that earth materials typically show larger resistivities when frozen than when unfrozen is well documented in the literature (2). The resistivity contrast between frozen and unfrozen sediments of the same type is the basis for the detection of permafrost using electrical methods.

The values of resistivity obtained from the interpretation created a basis for consideration of certain layers as frozen or unfrozen.

5.2 Relative and Absolute Coordinates

The interpretation of transient sounding data is mainly carried out by comparison of observed data to theoretical response of models. The theoretical response of the model can be expressed in either dimensionless parameters (relative coordinates - reference Figure 5) or in dimensioned parameters (absolute coordinates). The process of data interpretation at first determines as many parameters as possible for curve fitting using relative coordinate master curves. The reliability of the interpretation and identification of poorly defined parameters is then accomplished by comparison of the observed data and model response in absolute coordinates. In Section 6.0, the observed data and modelled

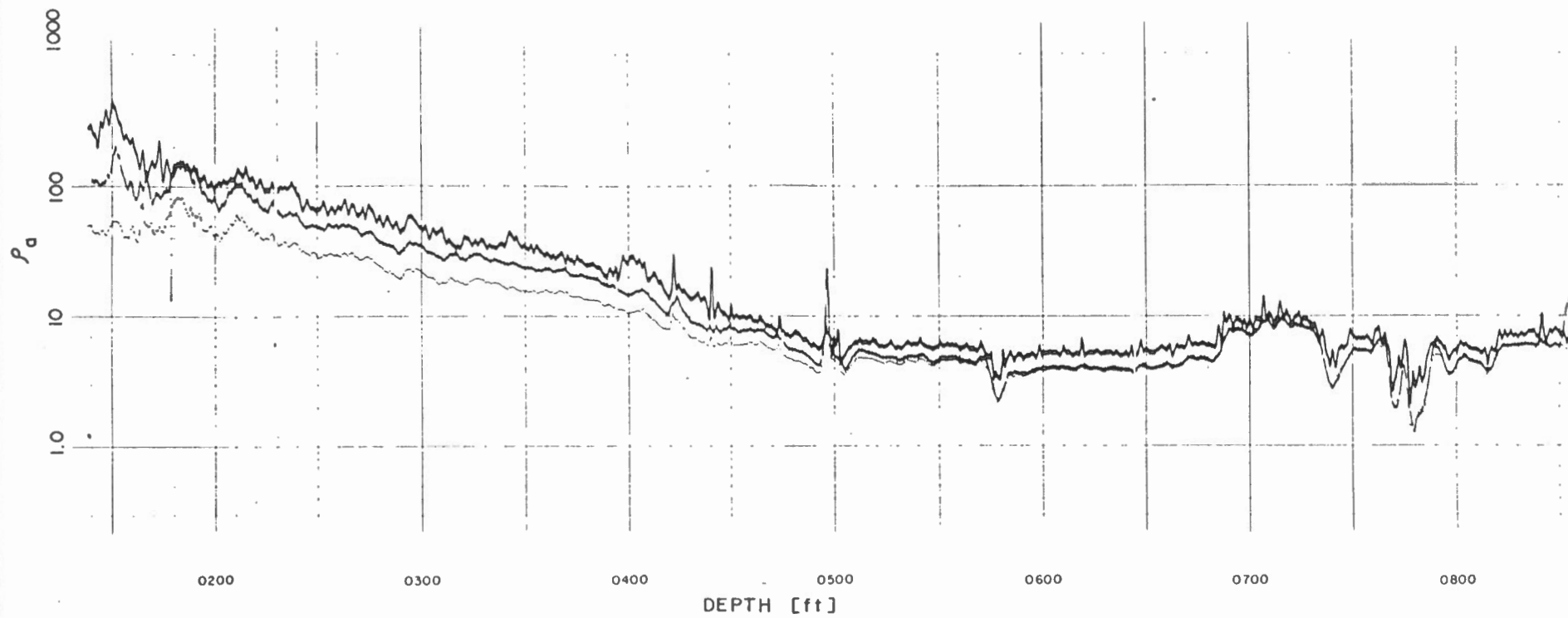
response are shown superimposed using the late stage apparent resistivity definition at several stations for both loop sizes.

5.3 The Description of Apparent Resistivity Curves

The curves obtained on land and off shore show substantially different behavior in accordance with the geoelectric sections to which they correspond.

5.3.1 Onshore Apparent Resistivity Curves

An example of an onshore curve is given in Figure 14 superimposed on the model curve. The curve shows a continuous decrease of resistivity with time. This corresponds to a decrease of the true resistivities with depth which can be seen in the resistivity logs available (Figure 11). In interpretation the continuous change of resistivity with depth was modeled by several layers having constant resistivity. For example, the model curve given in Figure 14 corresponds to the structure consisting of 5 layers. This explains slight deviations between the model and measured curves.



GEO-PHYSI-CON

EXAMPLE OF
RESISTIVITY LOG
DH B-44

C83-16

Figure 11

5.3.2 Offshore Curves

Figure 15 shows an example of offshore curves superimposed on the model curves. Both curves obtained with 100m by 100m and 500m by 500m loops have a left descending branch and then a minimum followed by an ascending branch. The left branches correspond to the ranges of time when the field measured has the early stage behavior. The minima and final ascending branches are due to the fact that the upper conductor is underlain by a resistor.

5.4 Distortions of the Apparent Resistivity Curves

All of the theory and the technique of interpretation of TEM sounding data is based on the assumption that the section consists of a number of layers separated by boundaries which are parallel to the surface. Of course, in the present survey this is not always the case. The presence of lateral inhomogeneities distorts more or less the apparent resistivity curves obtained. The question arises, which data (from either loop size) is subjected to stronger distortions.

There are two opposite effects. Lateral resolution can be expected to be better with the smaller loop size. Averaging ability is much stronger with the larger loop size, and therefore, some distorting effects can be expected to interfere and to purge each other.

Analysis has shown that the onshore curves obtained with 100m by 100m loops are distorted substantially at very early time channels. It was impossible to estimate quantitatively the degree of distortion, so that only the curves corresponding to 400m by 400m loops were used for the interpretation. The latter were also distorted at later time gates but it has been found that these distortions do not significantly affect the curve in the time range of interest.

Off shore curves were found not to be distorted.

5.5 Fixed Frequency EM Data

The fixed frequency data was gathered along the survey line using six different measurement modes. The quantitative interpretation of the data was impossible because of the complexity of the resistivity distribution within the upper 50m and the

absence of drill hole control. Due to these facts, fixed frequency profiles were used mainly qualitatively. The absolute values of the apparent conductivity were used to aid in the interpretation of TEM soundings.

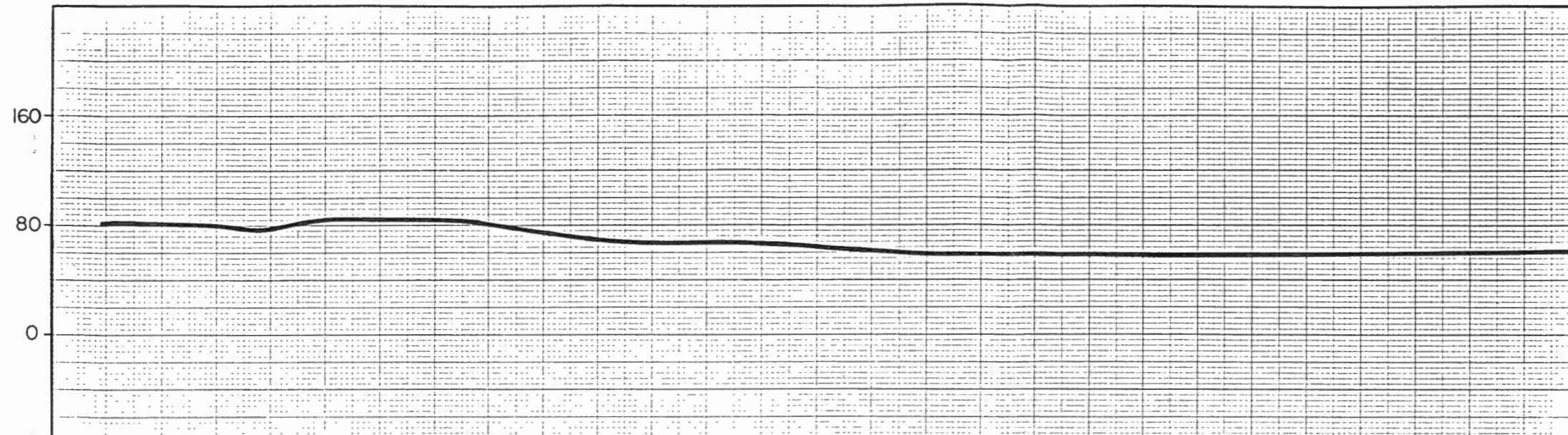
6.0 RESULTS

The fixed frequency profiles are given in Figures 12a to f. Drastic changes of apparent conductivity occur at the shore line.

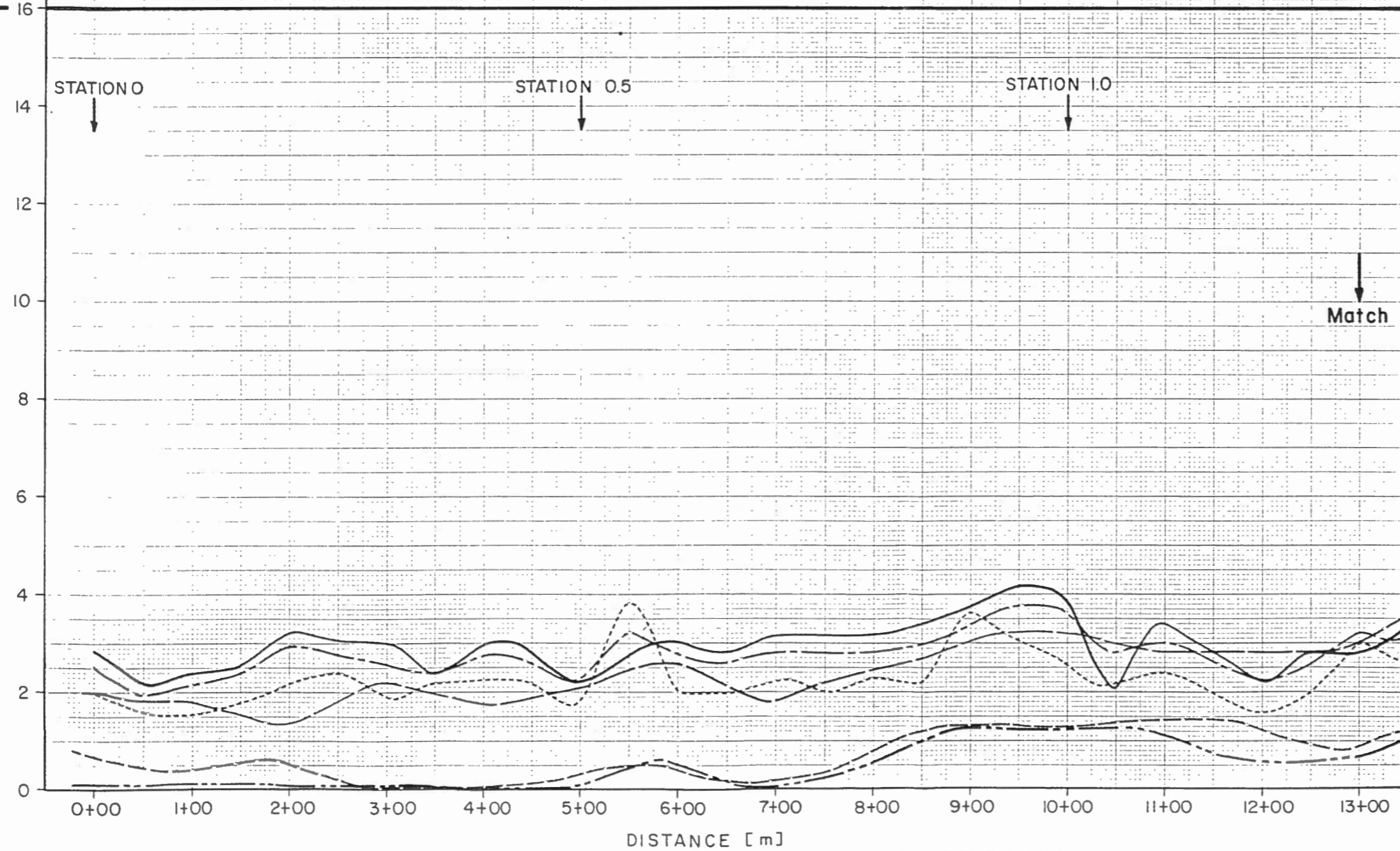
Figure 13 gives the section derived from the interpretation of apparent resistivity curves. The examples of fitting the measured and modelled curves are given in Figures 14 and 15.

Figure 13 shows the two types of structure along the survey line. Starting from Station 0, eastward, frozen ground has a thickness of about 200m. Approaching the shore line the depth to the bottom of permafrost becomes smaller and reaches a value of about 100m at Station 7.5.

HORIZONTAL CONTROL [m]



APPARENT CONDUCTIVITY [mmho/m]



LEGEND

- EM 34 (40 V)
- - - EM 34 (40 H)
- - - EM 34 (20V)
- EM 31 (HG)
- - - EM 31 (HZ)
- EM 31 (VG)

GEO-PHYSI-CON

FIXED FREQUENCY PROFILE

C83-16 Figure 12 a

HORIZONTAL CONTROL [m]

160

80

0

16

14

12

10

8

6

4

2

0

STATION 1.5

STATION 2.0

STATION 2.5

Match

Match

APPARENT CONDUCTIVITY [mmho/m]

13+00

14+00

15+00

16+00

17+00

18+00

19+00

20+00

21+00

22+00

23+00

24+00

25+00

26+00

27+00

DISTANCE [m]

LEGEND

- EM 34 (40 V)
- .-.- EM 34 (40 H)
- EM 34 (20V)
- EM 31 (HG)
- .-.- EM 31 (HZ)
- EM 31 (VG)

GEO-PHYSI-CON

FIXED FREQUENCY PROFILE

HORIZONTAL CONTROL [m]

160
80
0

APPARENT CONDUCTIVITY [mmho/m]

Match

STATION 3.0

STATION 3.5

STATION 4.0

Match

LEGEND

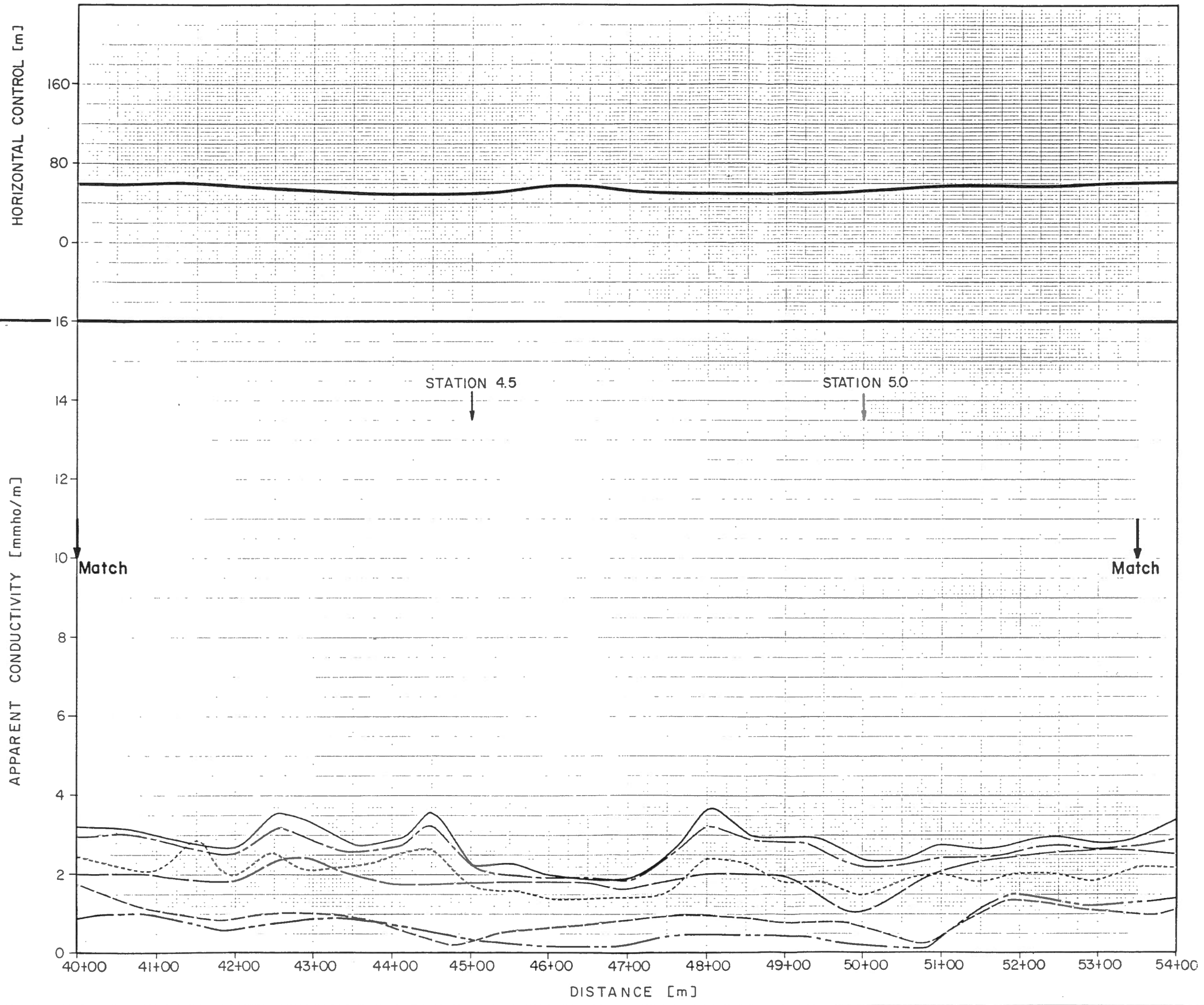
- · — · — EM 34 (40 V)
- · — · — EM 34 (40 H)
- · — · — EM 34 (20V)
- · — · — EM 31 (HG)
- · — · — EM 31 (HZ)
- · — · — EM 31 (VG)

GEO-PHYSI-CON

FIXED FREQUENCY PROFILE

27+00 28+00 29+00 30+00 31+00 32+00 33+00 34+00 35+00 36+00 37+00 38+00 39+00 40+00

DISTANCE [m]

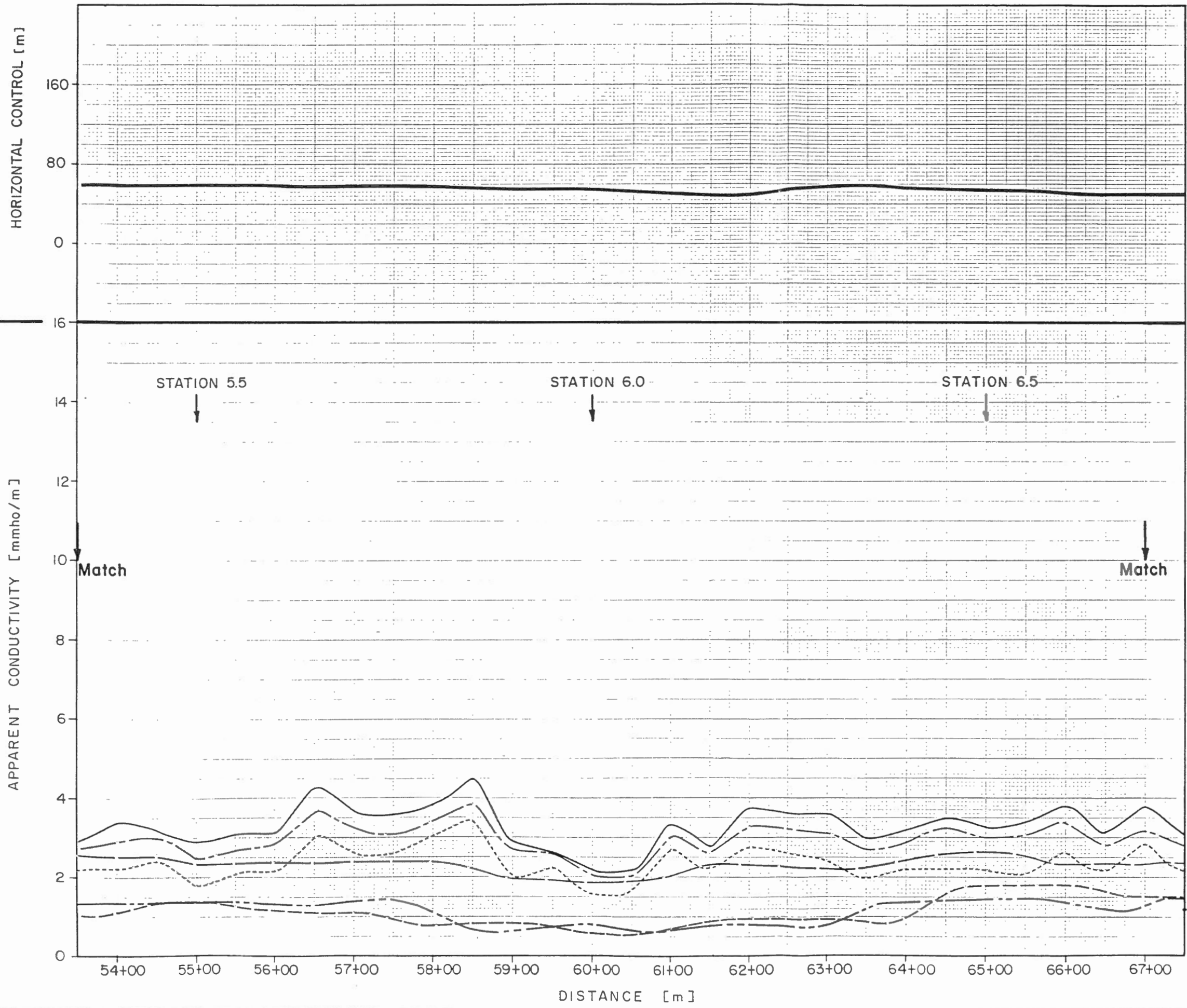


LEGEND

- EM 34 (40 V)
- EM 34 (40 H)
- EM 34 (20V)
- EM 31 (HG)
- EM 31 (HZ)
- EM 31 (VG)

GEO-PHYSI-CON

FIXED FREQUENCY PROFILE



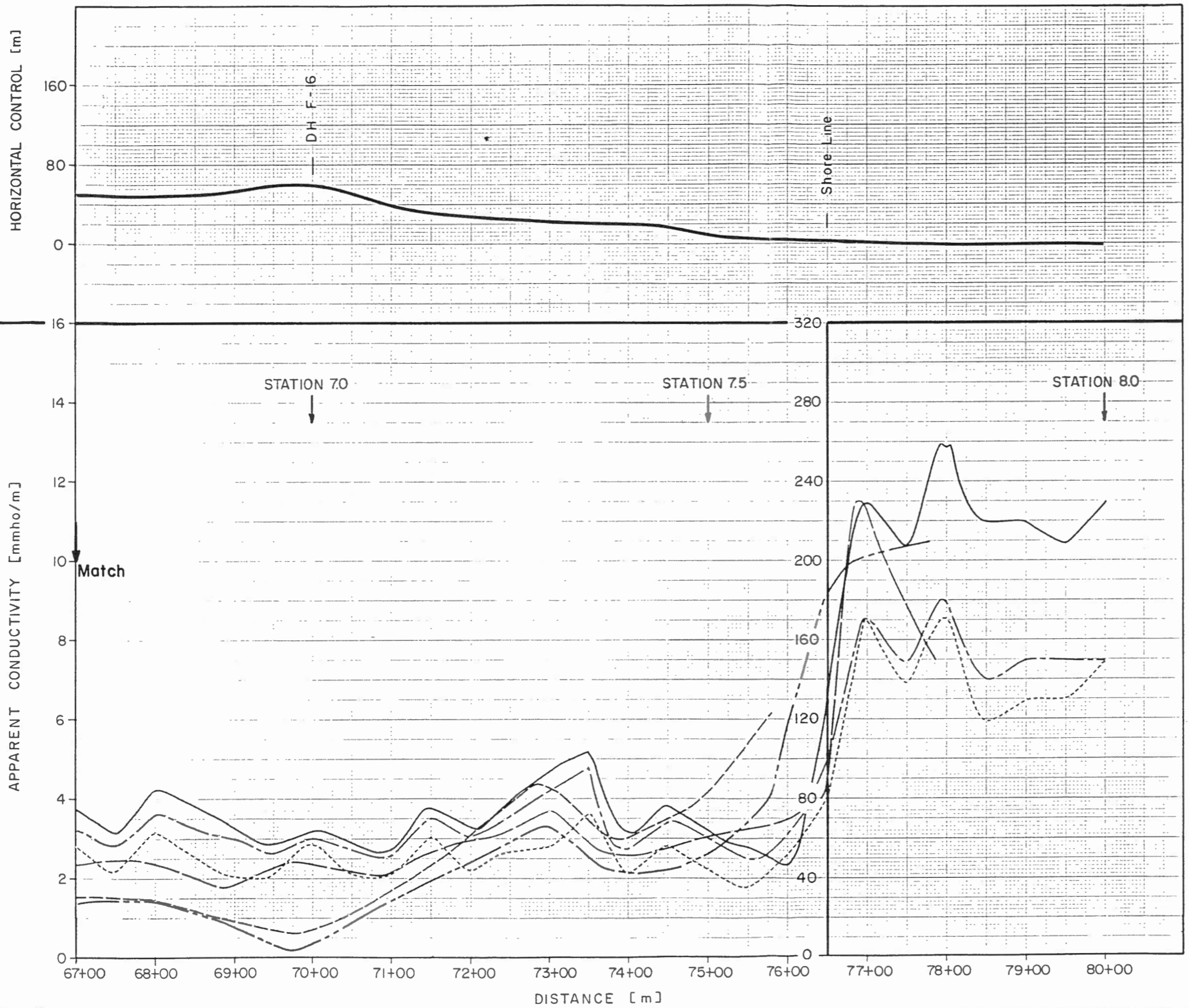
LEGEND

- EM 34 (40 V)
- - - EM 34 (40 H)
- · - EM 34 (20V)
- EM 31 (HG)
- - - EM 31 (HZ)
- · · EM 31 (VG)

GEO-PHYSI-CON

FIXED FREQUENCY PROFILE

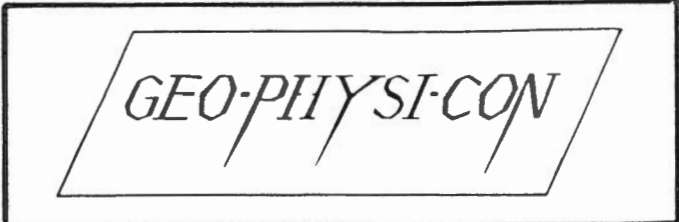
C83-16 Figure 12e



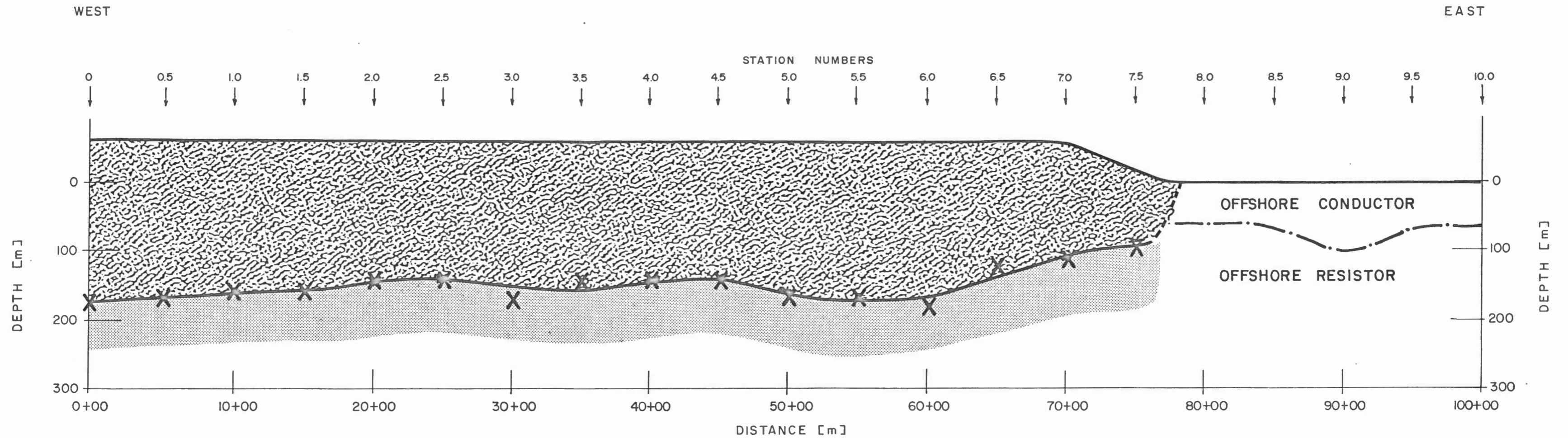
LEGEND

- EM 34 (40 V)
- - - EM 34 (40 H)
- EM 34 (20V)
- EM 31 (HG)
- - - EM 31 (HZ)
- EM 31 (VG)




NOTE :
Change in horizontal scale at
76+50 m.



FIXED FREQUENCY PROFILE



LEGEND

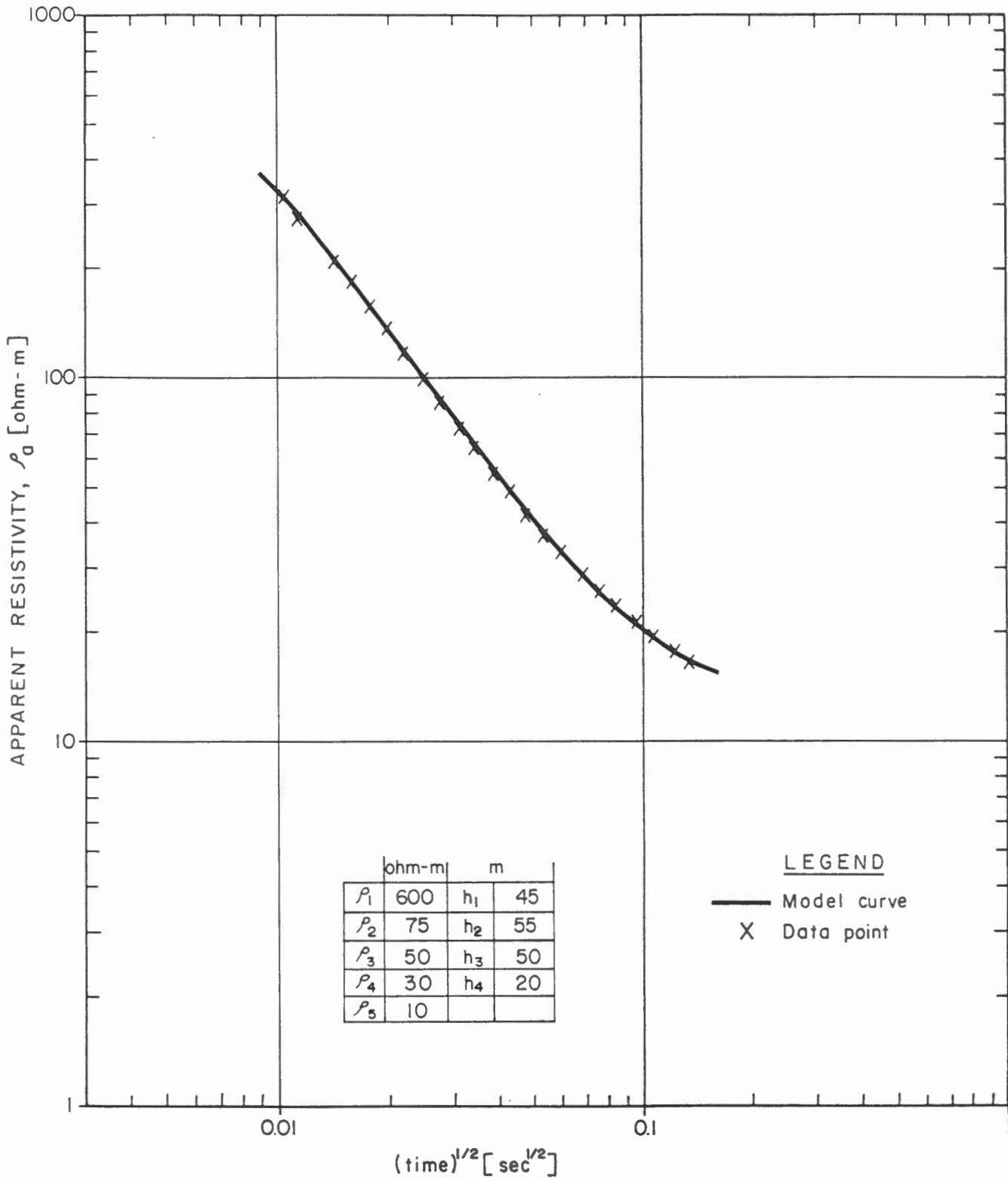
-  Frozen Ground
-  Unfrozen Ground
-  Top of Offshore Resistor

SCALE

Horizontal 1:25,000
 Vertical 1:5,000
 Vertical Exaggeration = 5 times

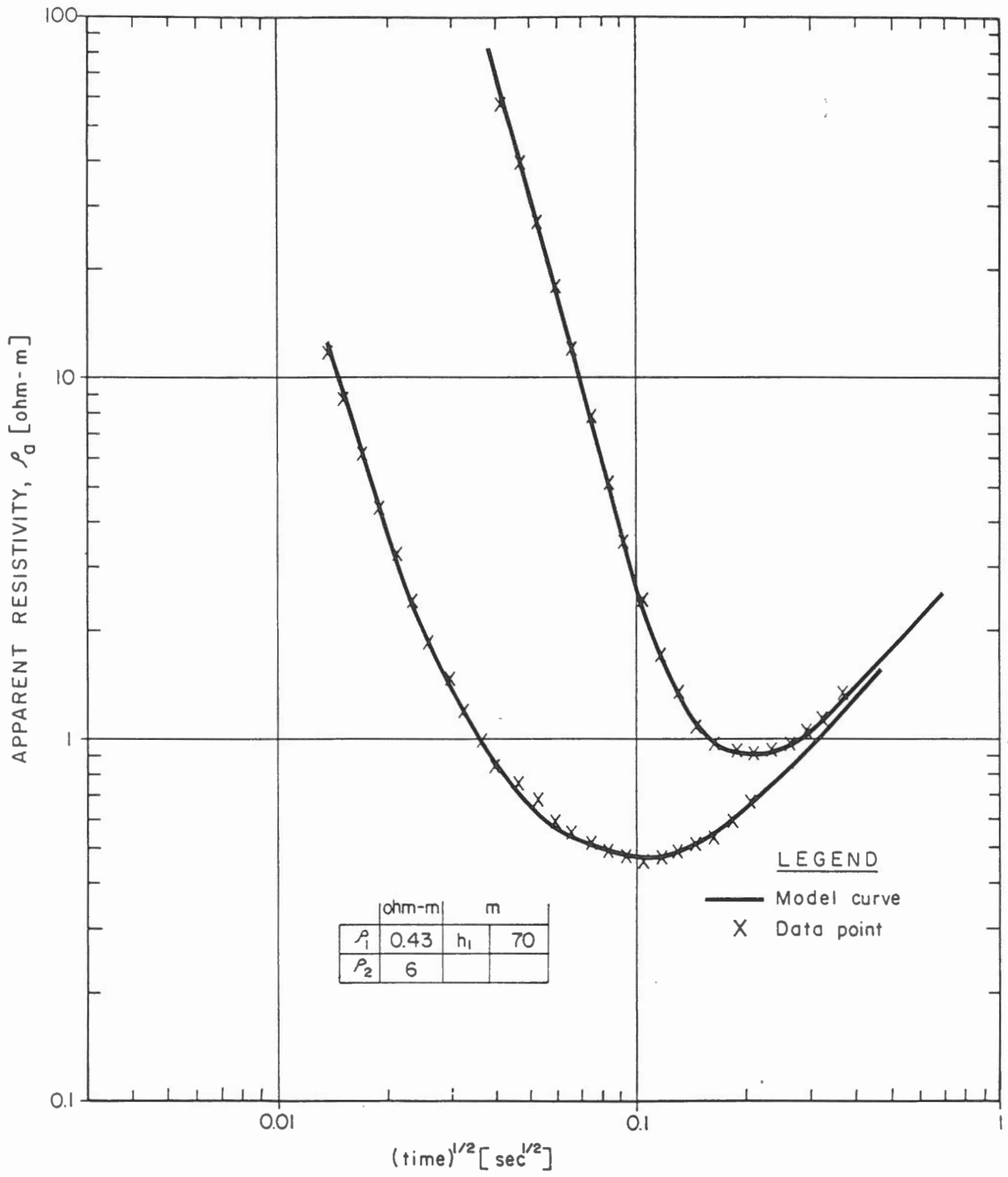
GEO-PHYSI-CON

EARTH PHYSICS BRANCH
 INTERPRETED SECTION
 DRAKE POINT



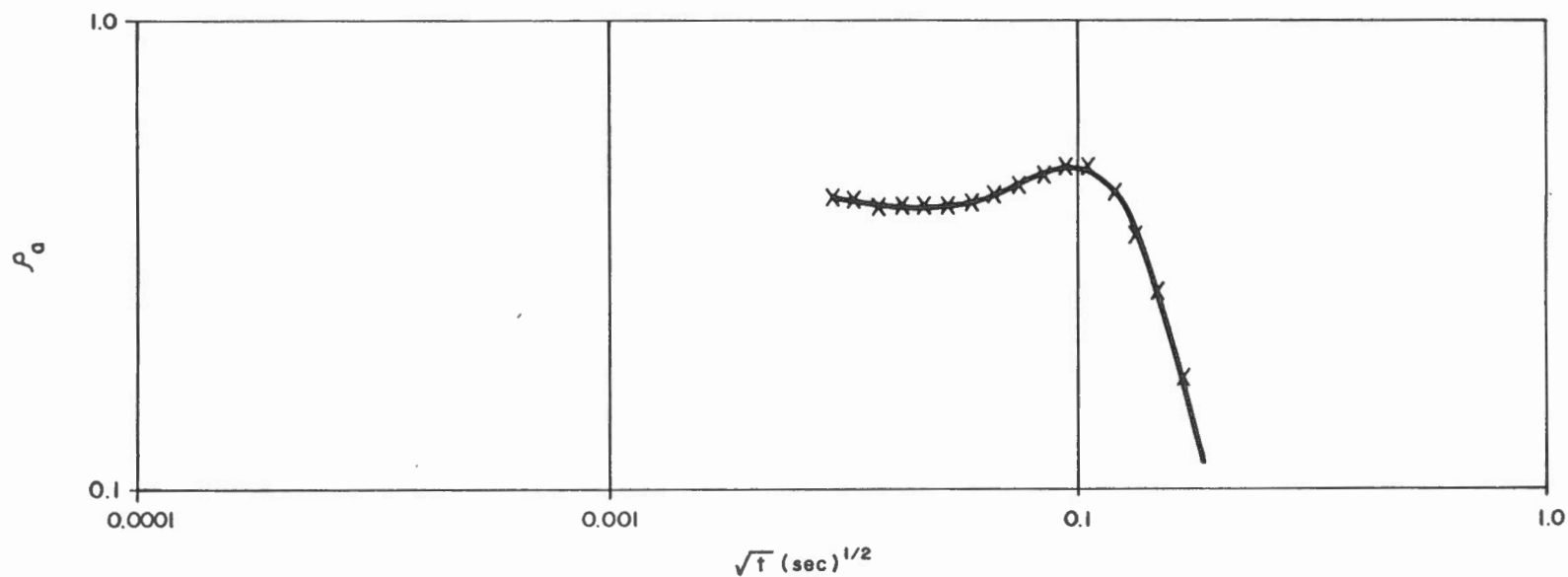
GEO-PHYSI-CON

TEM MEASURED AND
 MODELLED CURVES
 STATION 7



GEO-PHYSI-CON

TEM MEASURED AND
MODELLED CURVES
STATION 8.5

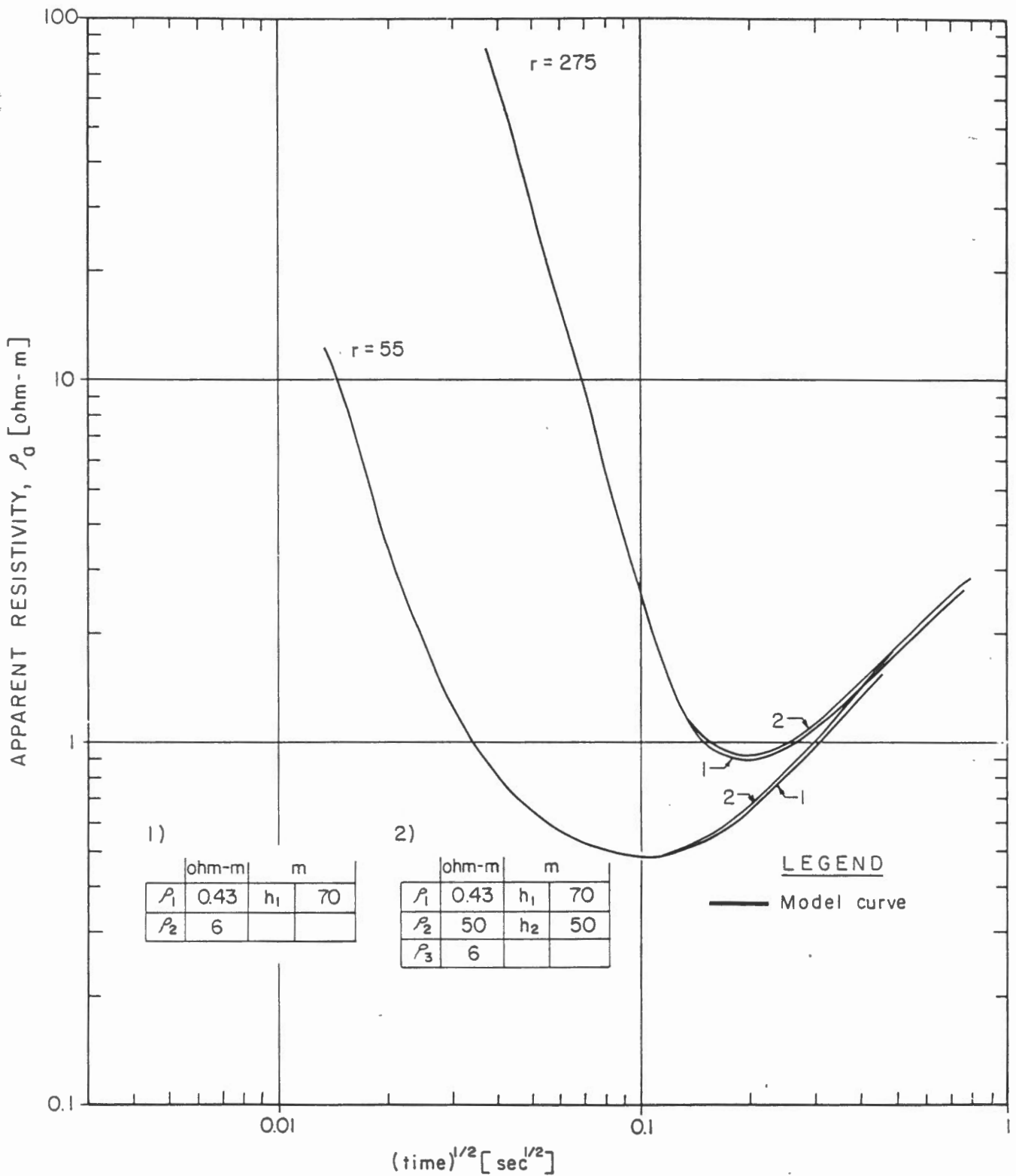


GEO-PHYSI-CON

EARTH PHYSICS BRANCH
 TEM EARLY STAGE CURVE
 STATION 8.5
 DRAKE POINT

C 83-16

Figure 16



GEO-PHYSI-CON

COMPARISON OF TEM CURVES
FOR SECTIONS
WITH AND WITHOUT
PERMAFROST

GEO-PHYSI-CON

Figure 14 shows data points superimposed on the model curve. Slight deviations can be explained by the fact that the continuous gradual decrease of resistivity with depth has been replaced with a layered model.

Starting from Station 8.0, eastward, the structure changes sharply and the shape of apparent resistivity curves changes drastically. Figure 15 shows the data points superimposed on the model curves.

The early stage curve obtained with the loop 500m by 500m is given in Figure 16. It is clearly seen from Figure 16 that the upper part has a nonuniform structure. As far as recovery of the layering within the upper part of the section was not an objective of this survey, the shallow layers (which are probably seawater) were approximated by a single layer. This explains the deviation of measured and model curves for the loop size of 100m by 100m. The vertical resolution of the large loop is less for shallower strata so that the effects of the replacement of upper layers by a single are essentially negligible.

The first off shore layer has a very low resistivity (0.4 to 0.5 ohm-m). Thus, a resistivity of 6 ohm-m, characteris-

tic for the underlying basement (as can be seen from the resistivity logs available) gives a resistivity ratio of 12 to 15. Figure 17 shows the curves corresponding to a two layered structure (sea water over basement) and to a three layered structure (sea water/permafrost/basement). It is evident that the difference between the curves is nonmeasurable. The problem of presence or absence of permafrost cannot be resolved unambiguously in the presence of very thick conductive layer. It is unlikely that any permafrost layer underlies 70m of sea water. If any frozen ground is present off shore its thickness would be expected to be less than 30m. The problem becomes resolvable when water depths decrease and/or permafrost thickness increases.

A trough in the top of the subsea resistor was found at Station 9.0.

7.0 CONCLUSIONS AND RECOMMENDATIONS

It can be concluded from the results of the survey that transient electromagnetic soundings are suitable for the investigation of permafrost distribution.

GEO-PHYSI-CON

A frozen section was found along the onshore portion of the survey line. The permafrost layer extended from the surface to depths varying from 230m in the west to 110m at the coast. The accuracy of determining the permafrost thickness is believed to be within 15%. This number should be verified by drilling.

A thick conductive layer with a resistivity of 0.4 to 0.5 ohm-m was encountered off shore. Its thickness varies from 70m to 100m. This layer represents sea water and, probably, a very upper portion of brine saturated sediments.

The conductive layer is underlain by a more resistive layer. It was impossible with the current system to determine whether any frozen material occurs off shore.

Employment of two transmitter loop sizes has proven to be very useful. The data obtained using a loop of smaller size were used both for better interpretation and for the analysis of lateral distortions.

Fixed frequency EM survey turned out to be very beneficial. This inexpensive method gives valuable information about shallow strata.

GEO-PHYSI-CON

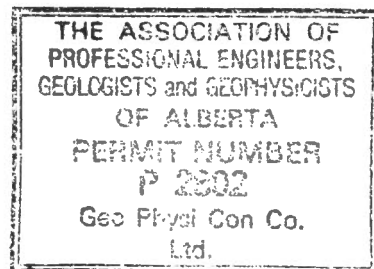
In the interest of planning of future surveys a number of recommendations can be made.

- i) The present survey was performed by one crew. Long daylight hours in the spring may allow use of two crew shifts to increase productivity.

- ii) For the present survey the vertical field of the transient electromagnetic response was measured. This field is, in general, proportional to conductivity to the power 1.5. Research has been underway over the last year to determine the usefulness of radial field data. The radial field is known to be proportional to the conductivity to a power of 2 and, therefore, contains more detailed information on the geoelectric section. The radial field data would be measured outside of the transmitter loop and would compliment vertical field data. The radial field has not been used for this purpose in the past and, and procedures for its use must be developed.

GEO-PHYSI-CON


iii) A weak signal strength limited the exploration depth under the specific geoelectric conditions encountered off shore. This can be remedied by transmitting greater current. A suitable generator is presently being sought.



Respectfully submitted,
GEO-PHYSI-CON CO. LTD.,

Per: 

W. H. G. Colles, B.Sc.
Project Geophysicist

Per: 

Grigory Rozenberg, M.Sc.
Senior Geophysicist

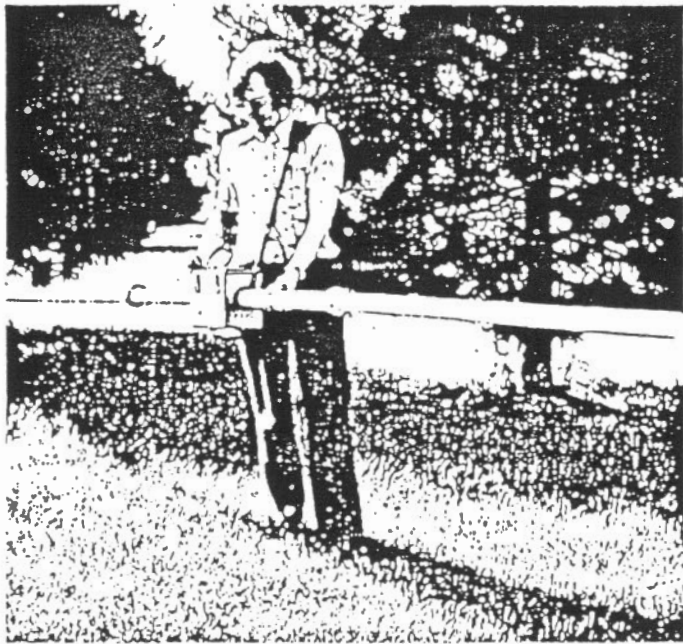
Per: 

T. Sartorelli, P.Eng.,
Senior Geophysicist

Calgary, Alberta
June 1983
C83-16

References

1. Kaufman, A. A., and Morozova, G. M. 1970. The theoretical basis of transient sounding in the near zone. Nauka, Siberian Division, Acad. Sci. U.S.S.R.
2. Hoekstra, P. and D. McNeill. Electromagnetic probing of permafrost. Proc. Second Int. Conf. on Permafrost, Yakutsh, U.S.S.R., North Am. Contrib. NAS-NAC, 479, 1973.



EM31

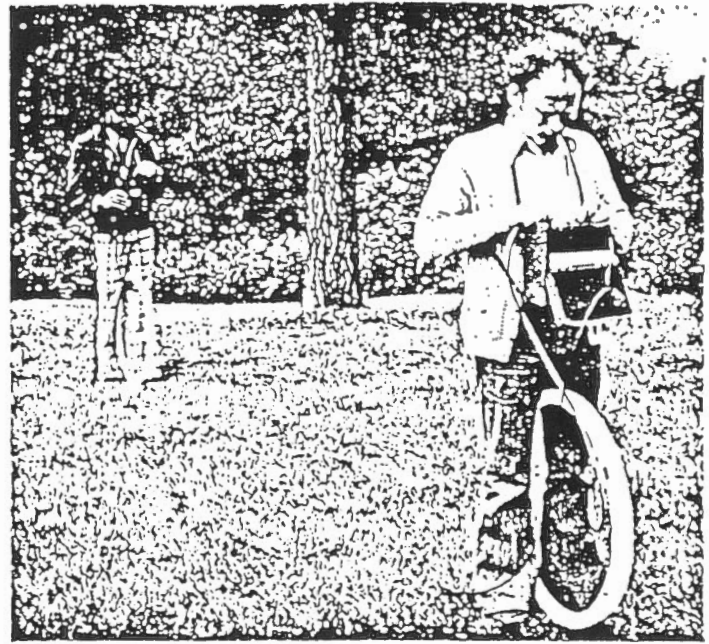
The Geonics EM31 provides a measurement of terrain conductivity without contacting the ground using a patented inductive electromagnetic technique. The instrument is direct reading in millimhos per meter and surveys are carried out simply by traversing the ground.

The effective depth of exploration is approximately six meters making it ideal for engineering geophysics. By eliminating ground contact, measurements are easily carried out in regions of high resistivity such as gravel, permafrost and bedrock. Over a uniform half space the EM31 reads identically with conventional resistivity and the measurement is analogous to a conventional galvanic resistivity survey with a fixed array spacing. Interpretation curves supplied with each instrument often permit an estimate of a layered earth.

The advantages of the EM31 are the speed with which surveys can be carried out, the ability to precisely measure small changes in conductivity, and the continuous readout which provides a previously unobtainable lateral resolution.

Specifications

MEASURED QUANTITY	Apparent conductivity of the ground in millimhos per meter.
PRIMARY FIELD SOURCE	Self-contained dipole transmitter
SENSOR	Self-contained dipole receiver
INTERCOIL SPACING	3.66 meters
OPERATING FREQUENCY	9.8 kHz
POWER SUPPLY	8 disposable alkaline "C" cells (approx. 20 hrs life continuous use)
CONDUCTIVITY RANGES	3, 10, 30, 100, 300, 1000 mmhos/meter
MEASUREMENT PRECISION	±2% of full scale
MEASUREMENT ACCURACY	±5% at 20 millimhos per meter
NOISE LEVEL	<0.1 millimhos per meter
OPERATOR CONTROLS	<ul style="list-style-type: none"> ● Mode Switch ● Conductivity Range Switch ● Phasing Potentiometer ● Coarse Inphase Compensation ● Fine Inphase Compensation
DIMENSIONS	Boom : 4.0 meters extended 1.4 meters stored Console : 24 x 20 x 18 cm Shipping Crate : 155 x 42 x 28 cm
WEIGHT	Instrument Weight : 9 kgm Shipping Weight : 23 kgm



EM34-3

Operating on the same principles as the EM31, the EM34-3 is designed to achieve a substantially increased depth of exploration and a readily available vertical conductivity profile.

The underlying principle of operation of this patented non-contacting method of measuring terrain conductivity is that the depth of penetration is independent of terrain conductivity and is determined solely by the instrument geometry i.e. the intercoil spacing and coil orientation. The EM34-3 can be used at three fixed spacings of 10, 20, or 40 meters and in the vertical coplanar (as shown) or horizontal coplanar mode. In the vertical coplanar mode, the instrument senses to approx. 0.75 of the intercoil spacing. In the horizontal coplanar mode, the instrument can sense to 1.5 times the intercoil spacing. For the horizontal coplanar mode, however, coil misalignment errors are more serious than in the vertical mode so greater care must be exercised to achieve the maximum 60 meter depth.

Simple operation, survey speed and straight forward data interpretation makes the EM34-3 a versatile and cost effective tool for the engineering geophysicist.

Specifications

MEASURED QUANTITY	Apparent conductivity of the ground in millimhos per meter
PRIMARY FIELD SOURCE	Self-contained dipole transmitter
SENSOR	Self-contained dipole receiver
REFERENCE CABLE	Lightweight, 2 wire shielded cable
INTERCOIL SPACING & OPERATING FREQUENCY	<ul style="list-style-type: none"> ● 10 meters at 6.4 kHz ● 20 meters at 1.6 kHz ● 40 meters at 0.4 kHz
POWER SUPPLY	Transmitter : 8 disposable "D" cells Receiver : 8 disposable "C" cells
CONDUCTIVITY RANGES	3, 10, 30, 100, 300 mmhos/meter
MEASUREMENT PRECISION	±2% of full scale deflection
MEASUREMENT ACCURACY	±5% at 20 millimhos per meter
NOISE LEVEL	<0.2 millimhos per meter
DIMENSIONS	Receiver Console : 19.5 x 13.5 x 26cm Transmitter Console : 15 x 8 x 26cm Coils : 63cm diameter
WEIGHTS	Receiver Console : 3.1 kg Receiver Coil : 3.2 kg Transmitter Console : 3.0 kg Transmitter Coil : 6.0 kg Shipping Weight : 41. kg

EM37 Ground Transient Electromagnetic System
Technical Specifications

Transmitter

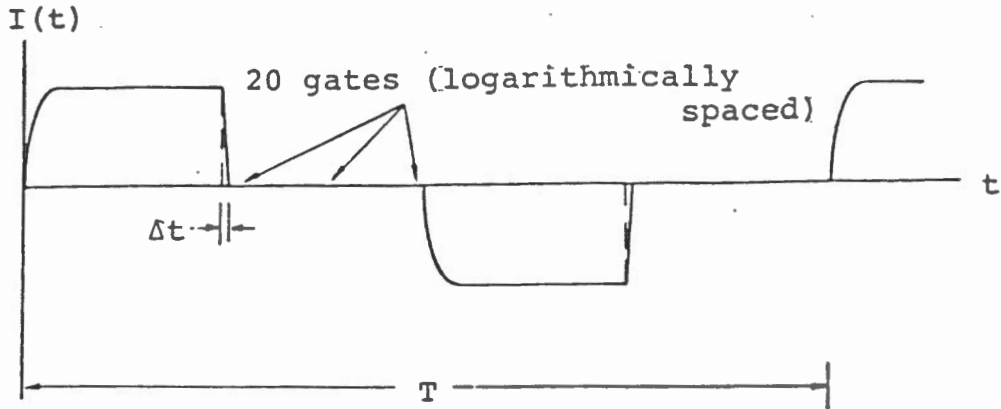
- | | |
|------------------------------|---|
| Current Waveform | - See Fig.A 1 |
| Repetition rate | - 3Hz or 30Hz in countries using 60Hz power line frequency; 2.5Hz or 25Hz in countries using 50Hz power line frequency; all four base frequencies are switch selectable. |
| Turn-off time (Δt) | - fast linear turn-off of maximum 300 μ sec. at 20 amps into 300x600m loop. Decreases proportionally with current and (loop area) ^{1/2} to minimum of 20 μ sec. Actual value of Δt read on front panel meter. |
| Transmitter loop | - any dimensions from 40x40m to 300x600m maximum at 20 amps. Larger dimensions at reduced current. Transmitter output voltage switch adjustable for smaller loops. Value of loop resistance read from front panel meter; resistance must be greater than 1 ohm on lowest voltage setting to prevent overload. |
| Transmitter protection | - circuit breaker protection against input over-voltage; instantaneous solid state protection against output short circuit; automatically resets on removal of short circuit. Input voltage, output voltage and current indicated on front panel meter. |
| Transmitter output voltage | - 150 volts (zero to peak) maximum;
20 volts (zero to peak) minimum |
| Transmitter output power | - 2.8 kw maximum |
| Transmitter wire supplied | - 1800m. #10 copper wire PVC insulated with nylon jacket; transmitter wire contained on 6 reels (supplied); 2 reel winders supplied. |
| Transmitter motor generator | - 5 HP Honda gasoline engine coupled to 120 volt, 3 phase, 400Hz alternator. Approximately 8 hours continuous operation from full (built-in) fuel tank. |

Receiver

- Measured quantity - time rate of decay of magnetic flux along 3 axes.
- Sensors - two air cored coils of bandwidths 11 and 50 kHz respectively; each 66cm dia.x4x5cm cross-section. Low frequency coil for general use, high frequency coil for shallow sounding.
- Time channels - 20 time channels with locations and widths as shown in Fig.A2. Successive operation at 30Hz, then 3Hz, effectively gives 30 channels covering range from 80 μ sec. to 80 msec.
- Output display - 4 figure digital LED plus sign; display also shows channel number and gain.
- Integration time - 2^n cycles at 30Hz; n=4,6,8,10,12,14 (switch selectable); similar integration times at other base frequencies.
- Receiver noise - approximately 1.5×10^{-10} volt/m²/turn of receiver coil at last gate at 30Hz with integration time of 34 seconds. Noise will be higher during intense local spherics activity.
- Output connector - all 20 channels available in analogue format from output connector at 5 volts fsd level.
- Synchronization to Tx - any of the following (switch selectable)
(1) reference cable
(2) primary pulse
(3) 27 MHz radio link (40 channels)
(4) high stability (oven controlled) quartz crystals.
- Noise rejection circuitry - with any of (1)-(3) above, entire system is automatically synchronized to 50/60Hz power line frequency when such interference exists in survey area; selective clipping of atmospheric noise pulses at all times. Audio output of Rx coil (transmitter pulse blanked out) is available on built-in loud speaker for ready identification of interference.
- Receiver batteries - 12 volt rechargeable Gel-cells; either 9 hours continuous operating time at 17°C (battery weight

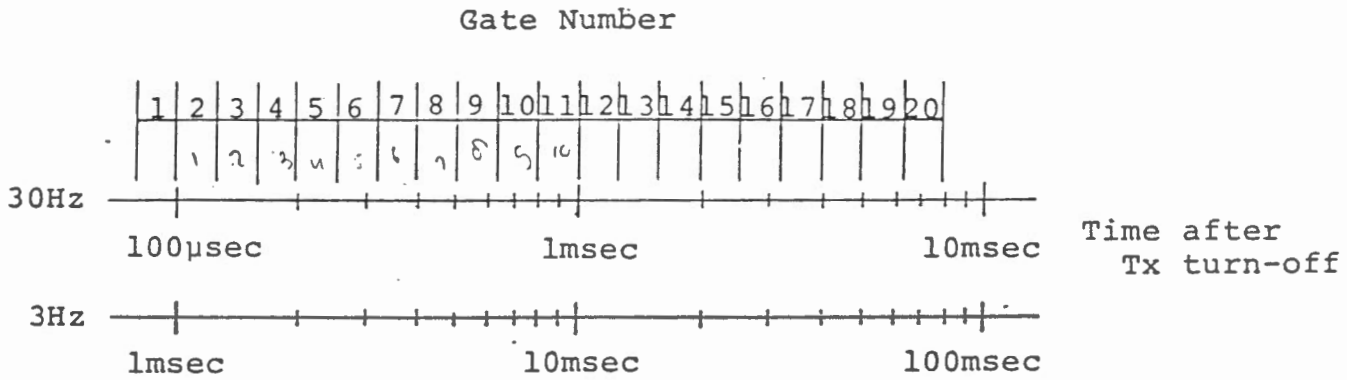
Receiver - Cont'd

Receiver batteries (continued) - battery weight 7.6 kg, 20 amp hour) or 2.5 hours continuous operating time (battery weight 2.6 kg, 6 amp hour). Two sets of batteries and a battery charger supplied to permit charging of spare set from transmitter motor-generator during survey.



Transmitter Current Waveform

FIG.A1



Gate Location and Widths (30 and 3Hz)

FIG.A2